European Journal of Medicinal Chemistry 271 (2024) 116429

Contents lists available at ScienceDirect

European Journal of Medicinal Chemistry

journal homepage: www.elsevier.com/locate/ejmech

Research paper

Exploring the modulatory influence on the antimalarial activity of amodiaquine using scaffold hybridisation with ferrocene integration

Mziyanda Mbaba [a], Taryn M. Golding [a], Reinner O. Omondi [a], Roxanne Mohunlal [a], Timothy J. Egan [a,1], Janette Reader [b], Lyn-Marie Birkholtz [b], Gregory S. Smith [a,*]

[a] Department of Chemistry, Faculty of Science, University of Cape Town, Rondebosch, 7701, South Africa
[b] Department of Biochemistry, Genetics and Microbiology, Institute for Sustainable Malaria Control, University of Pretoria, Hatfield, 0028, South Africa

ARTICLE INFO

Keywords:
Amodiaquine
Hybrid
Ferrocene
Malaria
Hemozoin inhibition

ABSTRACT

Amodiaquine (AQ) is a potent antimalarial drug used in combination with artesunate as part of artemisinin-based combination therapies (ACTs) for malarial treatment. Due to the rising emergence of resistant malaria parasites, some of which have been reported for ACT, the usefulness of AQ as an efficacious therapeutic drug is threatened. Employing the organometallic hybridisation approach, which has been shown to restore the antimalarial activity of chloroquine in the form of an organometallic hybrid clinical candidate ferroquine (FQ), the present study utilises this strategy to modulate the biological performance of AQ by incorporating ferrocene. Presently, we have conceptualised ferrocenyl AQ derivatives and have developed facile, practical routes for their synthesis. A tailored library of AQ derivatives was assembled and their antimalarial activity evaluated against chemosensitive (NF54) and multidrug-resistant (K1) strains of the malaria parasite, *Plasmodium falciparum*. The compounds generally showed enhanced or comparable activities to those of the reference clinical drugs chloroquine and AQ, against both strains, with higher selectivity for the sensitive phenotype, mostly in the double-digit nanomolar IC_{50} range. Moreover, representative compounds from this series show the potential to block malaria transmission by inhibiting the growth of stage II/III and V gametocytes *in vitro*. Preliminary mechanistic insights also revealed hemozoin inhibition as a potential mode of action.

1. Introduction

The strategy of incorporating dissimilar pharmacophoric units into a single chemical entity is increasingly gaining interest in contemporary drug discovery, with the goal of devising novel biological agents, that target multiple biological pathways to elicit their therapeutic efficacy [1–4]. This approach is particularly touted in research endeavours geared towards the elimination of parasitic infections. This is due to the alarming rate of rising resistance, of the causal agents of parasitic diseases, to current clinical drugs as front-line treatment options [2,3]. With the view of diversifying the mechanistic modality of bioactive drug molecules, researchers are turning their attention towards nonconventional organometallic chemotypes to expand the drug arsenal and potentially introduce innovative modes of action that are unrecognised to pathogenic strains responsible for the diseases [5,6]. Bioactive organometallic fragments bear many advantages compared to traditionally used organic drugs. They possess the capacity to interact with target biomolecules *via* complexation through the metallic centers and possess an enhanced affinity to bind to the 3-dimensional active sites of biological receptors or pockets owing to their inherent 3D geometry and better structural complementarity and recognition to bind to these cavities [7,8]. The practicality of this approach was reviewed by Cohen and Metzler-Nolte in which a cohort of selected metallo-fragments was shown to possess high binding affinity for pathologically relevant protein targets of various diseases, namely, Hsp90 (cancer), PA_N (viral infections) and NDM-1 (bacterial infections) [8].

The success of incorporating organometallic complexes into known drug scaffolds is exemplified by the discovery of antiproliferative ferrocifens and the potent antimalarial clinical candidate, ferroquine, reported by the research groups of Jaouen and Biot in the late 1990s, respectively [9,10]. These research groups incorporated the organometallic compound, ferrocene, into the scaffolds of the anticancer drug, tamoxifen, or antimalarial agent, chloroquine (CQ), to modulate their respective efficacies. In both cases, the presence of ferrocene was found

* Corresponding author.
E-mail address: gregory.smith@uct.ac.za (G.S. Smith).
[1] In memory of the late Prof. Timothy J. Egan.

https://doi.org/10.1016/j.ejmech.2024.116429
Received 25 February 2024; Received in revised form 13 April 2024; Accepted 15 April 2024
Available online 16 April 2024

to introduce novel mechanisms of action (e.g., intracellular generation of membrane-disruptive reactive oxygen species (ROS) by reversible Fenton-like processes) and enhanced the lipophilic character of the resulting compounds for better retainment in the active sites, thus improving their therapeutic value [11–13]. Consequently, a plethora of ferrocenyl bioactive conjugate compounds showing potency against a myriad of diseases, including anticancer [14–16], antimalarial [17–19], antibacterial, antiretroviral (HIV) and antitubercular activities [20–24], have since been generated and their biological and structure-activity relationship (SAR) profiles are well-delineated in the literature.

This strategy is of particular importance in malaria research due to the alarming threat of the development of resistant strains to current antimalarial drugs, such as chloroquine. This strategy offers an avenue to fashion novel compounds with diverse and, sometimes peculiar, modes of action that are not yet registered to the malaria parasite, and can potentially evade the development of clinical resistance. Of the five *Plasmodia* species responsible for malaria infections, *Plasmodium falciparum* (*P. falciparum*) and *Plasmodium vivax* (*P. vivax*) are the most prevalent. According to the WHO African region, 233 million cases were estimated in 2022, accounting for 93.6 % of the global cases [25]. Amodiaquine (AQ) is a quinoline-based drug partner of artesunate (AS) in the artemisinin-based combination therapies (ACTs) introduced by the WHO as a safeguard against clinical resistance development by malarial strains [26,27]. Although not widespread, AQ resistance, as well as the emergence of *P. falciparum* strains resistant to ACTs, have been recorded [28,29]. Thus, additional measures to contain the development of clinical resistance, for instance, by diversification of modes of action of current clinical drugs, is of worthy consideration in contemporary malaria research. While many amodiaquine analogues, including metallic complexes [30–33], have been explored in the literature [34–37], we could not find any accounts of ferrocene-based derivatives of AQ in our literature search.

Considering the rising threat of the development of resistance to current antimalarial medicaments and the fruitful developments in the hybridisation of known drug scaffolds with metallo-fragments, we endeavoured to interrogate the effect of incorporating ferrocene into amodiaquine, drawing inspiration from the success of ferroquine. Thus, the present study showcases the incorporation of the ferrocenyl entity to the scaffold of AQ in order to modulate its pharmacological profile with the goal of diversifying its mechanism(s) of action.

2. Results and discussion

2.1. Chemistry

Despite its high antimalarial potency, the use of AQ as a monotherapy is compromised by its severe side effects, ascribed to oxidative metabolic conversion into highly reactive, hepatotoxic quinoneimine (**A**) and aldehyde quinoneimine (**B**) metabolites, that takes place on the hydroxyl (OH) and diethyl amine (Et_2N) groups (Fig. 1) [38–41]. To address this drawback, O'Neill and co-workers have shown that incorporation of a bulky *N-tert*-butyl unit ($NHBu^t$) *in lieu* of Et_2N, as well as interchanging the positions of the OH and amine groups on the cresol motif led to less toxic and chemically labile AQ derivatives (i.e., isoquines) [42,43]. In our design strategy, ferrocene, a bulky metallo-fragment, was appended to the lateral amino side chain of AQ, replacing the diethyl amine motif, and the phenyl OH group was altered by substituting it with a hydrogen, to minimize biological oxidation of the resulting compounds into the reactive quinoneimine metabolites (Fig. 1). Lastly, the ferrocene unit was modified by attaching a methyl *N*, *N*-dimethylamine moiety ($R^2 = CH_2NMe_2$) to C-2 of the ferrocene unit, which is a critical structural feature in ferroquine.

The synthesis of the target compounds was carried out as illustrated in Scheme 1. Quinolinyl benzoic acids (**5a** and **5b**) were assembled by the reaction of appropriately substituted anilines, **1a** and **2a,** with 4,7-dichloroquinoline (**3**), *via* a facile S_NAr substitution reaction [44]. Compound **5a** was accessed straightforward by coupling commercially available aniline **1a** with **3**, while **5b** was effectively synthesized in four steps from nitrobenzoic acid (**1b**), which was first esterified, reduced (from NO_2 to NH_2, **2a**) [45], coupled to **3**, and subsequently hydrolyzed

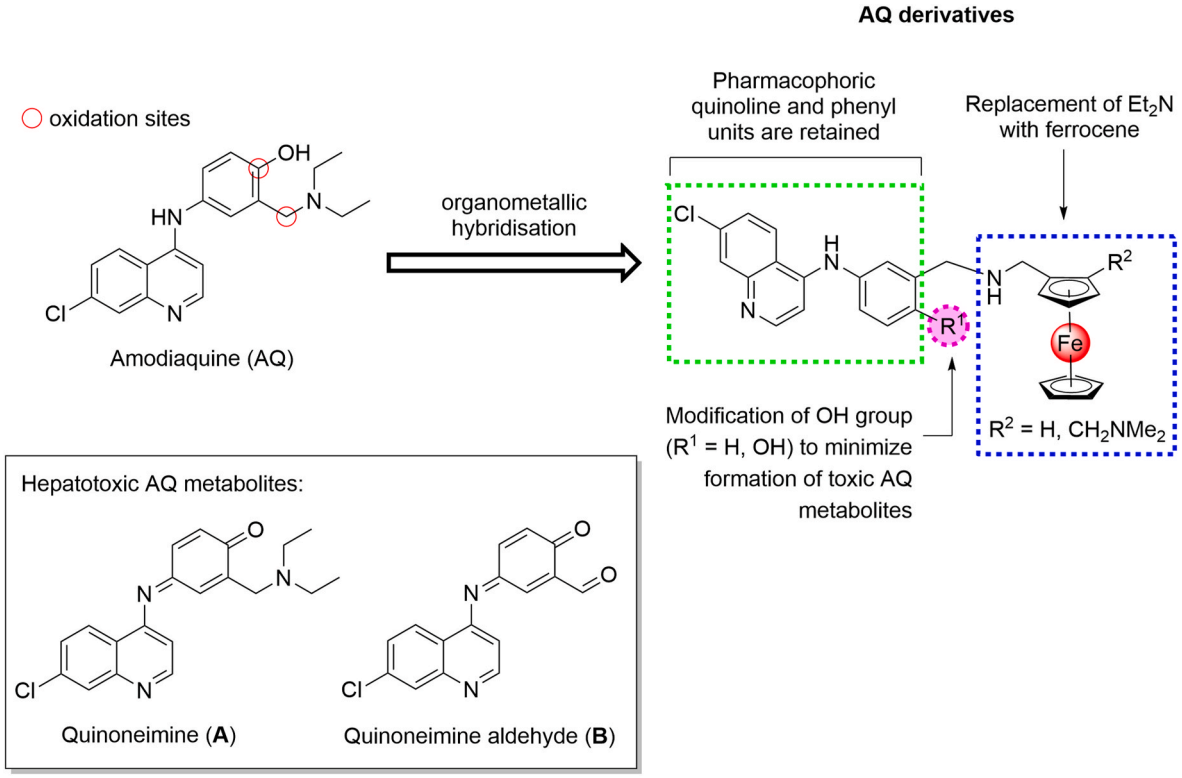

Fig. 1. Design strategy of ferrocenyl amodiaquine derivatives pursued in the present study.

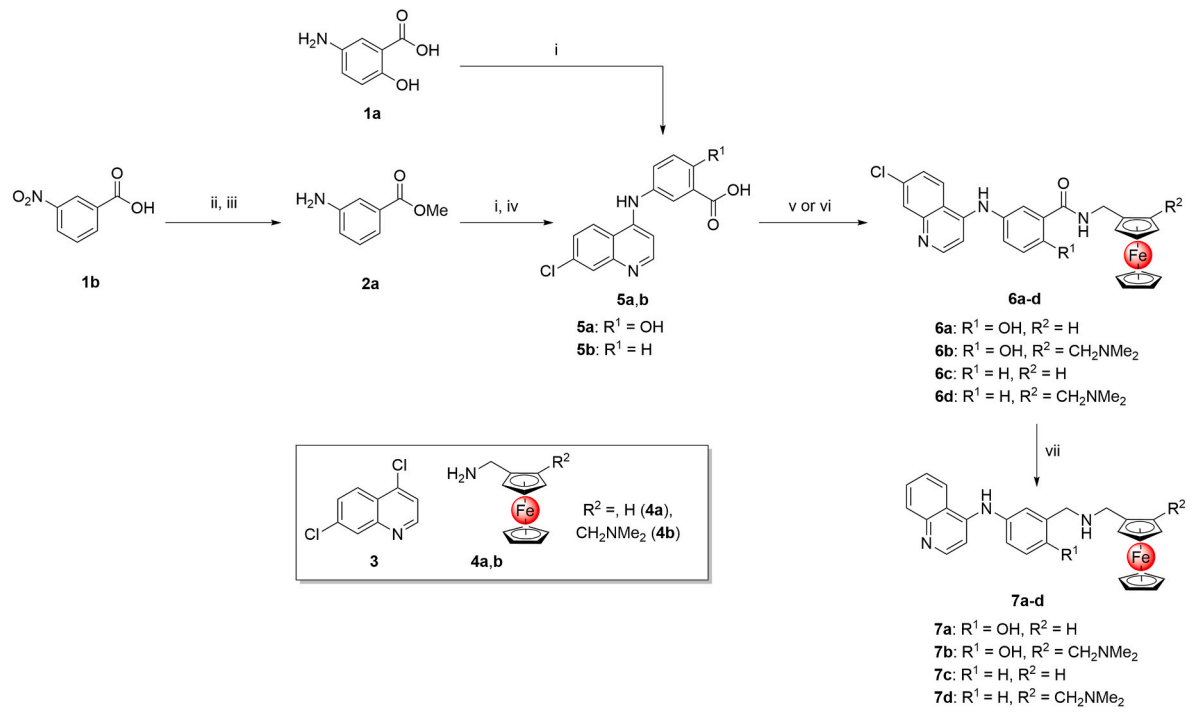

Scheme 1. Synthesis of amodiaquine derivatives. Reagents and conditions: (i) **3** (1.2 eq.), EtOH, reflux, 24 h; (ii) MeOH, cat. HCl (38 %), reflux, 24 h; (iii) Zn dust (5.0 eq.), sat. NH_4Cl, MeOH, reflux, 1 h; (iv) NaOH (3.0 eq.), 3:2:1 THF/MeOH/H_2O, reflux, 6 h (followed by an acidic workup); (v) **4a** or **4b** (1.0 eq.), DCC (1.2 eq.), pyridine, mw (200 W, 80 °C), 1 h; (vi) **4a** or **4b** (1.0 eq.), $P(OEt)_3$ (1.0 eq.), I_2 (1.0 eq.), Et_3N (2.0 eq.), DCM, Ar atm., r. t., 12–24 h; (vii) $LiAlH_4$ (5.0 eq.), anh. THF, Ar atm., reflux, 24–48 h.

to recover the carboxylic acid functional group. Condensation of the quinolinyl acids **5a** or **5b** with the relevant ferrocenyl amines (**4a** or **4b**), prepared according to reported literature procedures [10], under microwave irradiation (with DCC as a coupling agent) or $P(OEt)_3$-mediated amidation, furnished ferrocenyl quinoline amides **6a-6d** in yields of 41–97 % [46,47].

Amides **6a-6d** were reduced under anhydrous conditions using $LiAlH_4$ to yield the amines **7a-7d** in 45–74 % yields [48]. Surprisingly, all the amides (**6a-6d**) were transformed to the ferrocene-containing amodiaquines (**7a-7d**), coined ferrodiaquines in this paper, lacking the Cl group at position 7 of the quinoline moiety. We speculate that this could be due to the potent reducing strength of $LiAlH_4$ and the harsh conditions used, which led to the concomitant replacement of the 7-Cl group with a hydride. Attempts to reduce these amides under milder conditions, employing the TMSCl-$NaBH_4$ and Tf_2O–$LiAlH_4$ couples at room and sub-zero temperatures, were unsuccessful [49,50]. To circumvent the reduction step and retain the 7-Cl group on the ferrodiaquines, we used the Mannich condensation protocol by coupling quinolinyl phenol **8** (prepared from **3** and 4-hydroxyaniline **2b**) and ferrocenyl amines **4a** or **4b**, with 10 equivalents of paraformaldehyde, in the presence of LiCl as a Lewis acid, to yield the 7-chlorinated ferrodiaquines **9a** and **9b** (Scheme 2) [51]. Interestingly, the reaction with ferrocenylamine **4a** led to concomitant formation of the benzoxazine analogue **9c** in a yield of 13 %. This analogue could be easily hydrolyzed to its aminocresol congener, ferrodiaquine **9a**, with aqueous citric acid.

The target ferrodiaquine amides (**6a-6d**) and amines (**7a-7d**, **9a-c**) were characterized using common spectroscopic techniques; ^1H and $^{13}C\{^1H\}$ NMR spectroscopy, IR spectroscopy and high-resolution mass

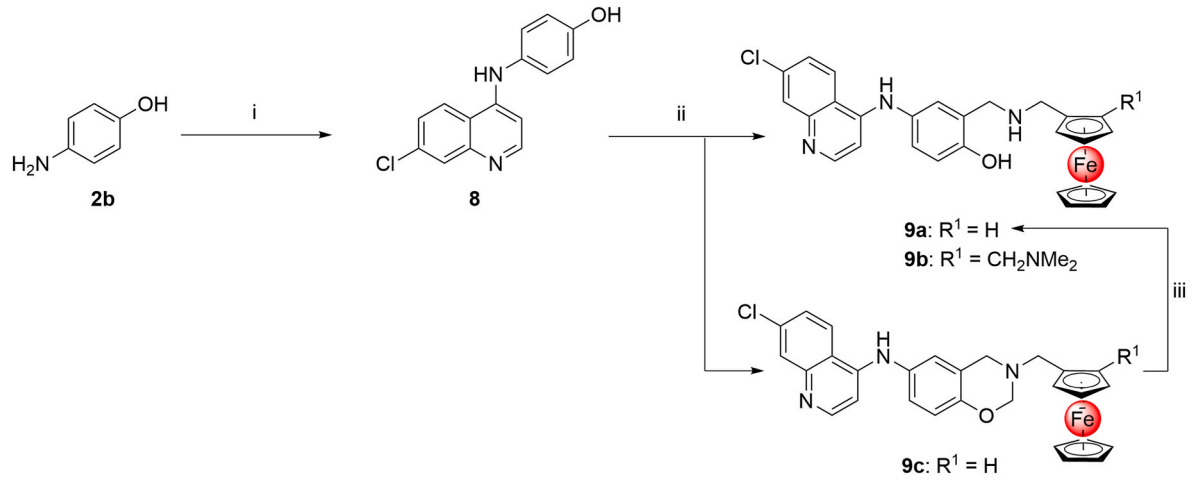

Scheme 2. Synthesis of 7-chlorinated ferrodiaquines **9a**,**b**. Reagents and conditions: (i) **3** (1.2 eq.), EtOH, reflux, 24 h; (ii) **4a** or **4b** (1.0 eq.); paraformaldehyde (10.0 eq.), LiCl (1.0 eq.), Et_3N (1.0 mL), EtOH, reflux, 12 h; (iii) 10 % aq. citric acid solution, EtOH, reflux, 2 h.

spectrometry (HRMS). The characteristic signals of ferrocene resonate between δ_H 4.29–4.03 ppm and δ_C 84.8–65.7 ppm in the ^{1}H and ^{13}C NMR spectra of the compounds, respectively, while the quinoline and phenyl units were confirmed by their signals in the aromatic region. Noteworthy, ferrocenyl amides (**6b**,**6d**) and amines (**7b**, **7d** and **9b**), containing a basic methyl *N*,*N*-dimethylamine side chain (R = CH_2NMe_2), show geminal coupling of the two CH_2 protons in the aliphatic region, due to planar chirality of the substituted ferrocene [52], which were observed as four doublets, each integrating for 1H, with *J*-coupling constants of 10.0–13.7 Hz, in their distinctive regions as previously noted in the literature [12,53]. On the other hand, the methylene protons (CH_2) for amides **6a** and **6c** were observed as either a 2H singlet (**6c**) or multiplet (**6a**) at δ 4.29 and 4.22 ppm, respectively, while two 2H singlets corresponding to the two CH_2 groups were observed in the range δ 3.85–3.56 ppm in the ^{1}H NMR spectra of the amine variants **7a** and **7c**. The *O*–CH_2–*N* functionality in benzoxazine **9c** was observed at its distinctive chemical shift (δ_H = 4.86 ppm), as previously observed for other ferrocenyl benzoxazine-type compounds. Assignment of proton signals was achieved by multiplet analysis and 2D NMR techniques; COSY, HSQC and HMBC (on representative compounds). The absence of the carbonyl amide carbon around δ 167.0 ppm (^{13}C NMR spectra of **6a-6d**) and the appearance of a new CH_2 signal in the ^{13}C NMR spectrum of amines **7a-7d** confirmed successful reduction of amides **6a-6d**. The proton at position 7 of compounds **7a-7d** was observed as a triplet in the ^{1}H NMR spectra of these compounds (δ_H 7.65–6.68 ppm), whereas the shielding of the ^{13}C NMR signal for C-7 (from δ 134.0 to 130.0 ppm) validated the absence of the Cl group. These observations were further corroborated by the IR data of amines **7a-7d**, which showed no presence of the characteristic C=O amide absorption band between ν1630 to 1780 cm^{-1}.

2.2. Asexual blood-stage antiplasmodial activity

The synthesized quinolinyl acids (**5a** and **5b**), the amide ferrodiaquines (**6a** - **6d**), and the amine ferrodiaquines (**7a** - **7d** and **9a** - **9b**) were assessed for their *in vitro* asexual blood stage antiplasmodial activity against the chloroquine-sensitive (NF54) and -resistant (K1) *P. falciparum* strains, using the *Plasmodium* lactate dehydrogenase (*p*LDH) assay [54]. The antiplasmodial activity was quantified as the concentration of compound required to inhibit the growth of the parasites by 50% of the initial population (i.e. half-maximal inhibitory concentration (IC_{50})). The results are summarized in Table 1.

The majority of the tested ferrodiaquines show activity in the submicromolar region against both the sensitive and resistant strains of *P. falciparum*. Of the 11 tested ferrodiaquines, ferrodiaquine **6a** (IC_{50} = 1.0216 ± 0.1695 μM) and its amine congener **9a** (27.4403 ± 7.1834 μM) were the only compounds to not show activity in the submicromolar range against the NF54 parasites. The aforementioned complexes, as well as **6c**, were also the only compounds to display IC_{50} values > 1 μM, against the resistant strain. Ferrodiaquines **7a**, **7b**, and **9b** demonstrated potencies superior to the clinical control drug, CQ (IC_{50} = 38.4 nM), and were the only compounds to show comparable activities to the parental drug AQ (IC_{50} = 20.9 nM) against the chemosensitive NF54 strain. More notably, however, **7a** and **9b** are at least five-times more potent than CQ against the resistant form of the parasite and **7a**, in particular, is nearly three-times more potent than AQ in the resistant K1 strain. Remarkably, complex **7a** displays comparable activity to FQ in the NF54 strain and is slightly more potent than FQ in the resistant K1 strain.

Generally, the tested compounds appeared to be more selective for the CQS strain (NF54), over the multidrug-resistant variant (K1), as attested by the resistant indices of >1. Despite the RI values exceeding one in some cases, it is worth noting that all of the tested compounds, barring complex **6c**, have resistance indices less than CQ, suggesting that these complexes will display mild cross-resistance, but not to the same extent as CQ. Moreover, not only is **7a** superior in activity to AQ and FQ in the CQR K1 phenotype, but it showed no cross-resistance (RI < 1), whereas AQ and FQ have RI values of 2.33 and 1 respectively. Although with inferior potencies, a lack of cross-resistance was also observed for **6d** and **9c**. With the exception of **6a**, **6c**, **7d**, and **9a**, the ferrodiaquines performed better than CQ on the K1 variant.

Furthermore, the quinolinyl acids **5a** and **5b**, which lack the ferrocenyl moiety, were significantly less active in both strains, than the subsequently synthesized ferrocenyl complexes. This increase in potency observed upon integration of the ferrocenyl group, further highlights the pharmacological significance of the ferrocene unit and lends impetus to the hybridisation strategy of organic drug scaffolds with metallofragments as a viable avenue to modulate the activity of known antimalarials, as reported in the literature [10,46]. A similar trend was observed for the phenol precursor **8**, which also lacks the ferrocene unit, and ferrocenyl complexes **9b** and **9c**.

In general, this structure-activity relationship (SAR) analyses suggests that the incorporation of the ferrocene unit into the lateral phenyl ring of the amodiaquine scaffold is indeed favourable for antimalarial activity (*cf.* acids **5a**, **5b** vs ferrodiaquines **6a-6d, 7a-7d**) (Table 1). Substitution at position C-2 of the ferrocene unit, with the CH_2NMe_2 chain, was beneficial for the activity of the ferrodiaquine amides (**6a-6d**) in both strains (e.g. IC_{50} (NF54) = 1022 nM (**6a**) *vs.* 51.4 nM (**6b**)). For the ferrodiaquines amines (**7a-7d**), however, the CH_2NMe_2 side chain seemed to have no effect in the NF54 strain, but its incorporation reduced the potency of the compounds against the K1 strain (e.g. IC_{50} (K1) **7a** *vs.* IC_{50} (K1) **7b**). The presence of the carbonyl group at the α-carbon of the phenyl ring (i.e., amides **6a-6d**) seemed to effect lesser

Table 1
In vitro antiplasmodial activity of the precursors (**5a**, **5b**, and **8**) and the corresponding ferrodiaquines (**6a-6d**, **7a-7d**, **9a-9c**) against the CQS NF54 and multidrug-resistant (K1) strains of *P. falciparum*, their aqueous solubility, and *c*LogP values.

Compound	IC_{50} ± SD (nM)		[a]RI	Aqueous solubility pH 6.5 (μM)	[b]cLogP
	NF54	K1			
5a	>20 000	>40 000	1.40	[c]n.d.	[c]n.d.
5b	>200 000	>200 000	0.70	[c]n.d.	[c]n.d.
6a	1021.6 ± 169.5	1387.0 ± 159.3	1.36	<5	6.0
6b	51.4 ± 5.2	63.9 ± 12.8	1.24	10	5.9
6c	447 ± 5.2	17 880 ± 1200	40.0	[c]n.d.	5.5
6d	65.9 ± 21.8	61.2 ± 9.4	0.93	90	5.6
7a	19.6 ± 1.53	19.0 ± 1.46	0.97	45	5.2
7b	20.1 ± 2.3	105.0 ± 8.1	5.22	<5	5.3
7c	39.0 ± 12.7	102.9 ± 23.6	2.64	170	5.5
7d	43.1 ± 10.6	319.2 ± 69.2	7.41	[c]n.d.	5.6
8	555 ± 41.7	727 ± 83.4	1.31	[c]n.d.	[c]n.d.
9a	>20 000	>20 000	0.83	20	5.8
9b	23.7 ± 2.82	58.4 ± 7.30	2.46	15	5.9
9c	145 ± 17.3	66.6 ± 2.65	0.46	20	6.3
AQ	20.9 ± 2.36	48.8 ± 8.84	2.33	[c]n.d.	[c]n.d.
[d]**CQ**	38.4 ± 8.6	307.4 ± 108.2	8.01	[c]n.d.	[c]n.d.
[e]**FQ**	20.2 ± 2.6	23.9 ± 0.18	1	[c]n.d.	[c]n.d.

[a] RI, resistance index = IC_{50}(K1)/IC_{50}(NF54).
[b] *c*LogP, calculated LogP according to reported literature methods [55].
[c] n.d., not determined.
[d] CQ, activity of chloroquine tested as a diphosphate salt.
[e] FQ, from literature [19].

potency against the NF54 strain compared to its methylene counterpart (i.e., amines **7a-7d**). This trend is generally reversed for the K1 phenotype. An interpretation of this observation suggests that the free rotation of the α-C—N bond plays a crucial role in discriminating between the two malarial phenotypes. It is speculated that the presence of the amine group (NH in amines **7a-7d**) plays a crucial mechanistic role in the activity of the compounds, e.g., by providing more sites for protonation, resulting in better accumulation and retention of the molecules in the active site of the NF54 parasites (digestive vacuole) [56]. This would imply that this effect is off-set, for instance, by drug resistance mechanisms, in the multidrug-resistant K1 phenotype, hence the reduced activity. Lastly, the presence of the hydroxyl group (OH) on the lateral benzene ring did not seem to have an obvious effect on the antimalarial activity of the amide ferrodiaquines (**6a-6d**). However, its incorporation was noted to enhance the activity of the amine ferrodiaquines (**7a-7d**) at least two-fold. Furthermore, the phenolic acid **5a** was found to be more active than its non-phenolic congener **5b**, in both strains. From this, we could infer that intramolecular hydrogen bonding through the phenolic OH may have pharmacological implications for this class of compounds, a phenomenon beneficial for other phenolic antimalarial agents reported in the literature [57,58].

2.3. Sexual gametocytocidal antiplasmodial activity

Antimalarial drugs that are active at different stages of the *P. falciparum* life cycle are becoming increasingly important in malaria drug discovery. A long-lived drug, targeting the parasite at different stages of its life cycle, has the potential to offer a single-dose cure as it can clear parasitemia at both the sexual and asexual stages of development. In view of this, selected ferrodiaquines were assessed for their inhibitory activity against *P. falciparum* gametocytes at immature and mature developmental stages (Table 2). Representative ferrodiaquines, **6d** and **7a**, exhibited single-digit low-micromolar potencies against immature gametocytes, while **7b** was relatively inactive. The mature gametocytes seem to show limited sensitivity towards the compounds, with activities above 10 μM. Though at a lower potency, *vis-à-vis* the asexual trophozoite stage (NF54 and K1), it is evident that the ferrodiaquines exert plasmocidal effects on the sexual stage parasites. Reduced potency against mature gametocytes, relative to the asexual stage, is a common observation for compounds targeting hemozoin formation, as reported for several antiplasmodial compounds in the literature [59–61]. This illustrates the potential of these compounds to inhibit the growth of the malaria parasite at different stages of its life cycle. This data therefore supports our proposed mechanism of action (*vide infra*) regarding inhibition of hemozoin formation. The mature gametocytes have lost the ability to do this, and only immature gametocytes can process heme into hemozoin. The gametocytocidal antiplasmodial activity data then supports that this is still happening in immature gametocytes, but since mature gametocytes do not have this ability, a loss in activity is observed.

2.4. Putative mechanism of action

Following the evaluation of the compounds for antiplasmodial activity, we undertook preliminary mechanistic studies to gain insight into a plausible mode of action of the investigated ferrodiaquines. There is ongoing evidence supporting the well-established theory that hematin remains the molecular target of quinoline antimalarials. As a consequence, the ability of the compounds to interact with hematin was assessed and the results are summarized in Table 3.

2.4.1. β-Hematin inhibition studies

Of the synthesized ferrodiaquines, amides **6a**, **6b**, and **6d**, amines **7a-7d**, and the chlorinated amines **9a-9c**, which showed promising antiplasmodial activity, were further probed to explore their potential mode of action using the cell-free detergent-mediated β-hematin inhibition assay [62,63]. A prominent study has demonstrated that when *Plasmodium*-infected red blood cells were inoculated with 4-aminoquinolines, namely, chloroquine and amodiaquine, at single-dose concentrations higher than their IC_{50} values, there were notable increases in the levels of 'free-heme' and a concomitant decrease in the amount of hemozoin formed [64]. This further supports the notion that quinolines do inhibit the biocrystallisation of free heme to inert hemozoin within the parasite's acidic digestive vacuole.

Quinolines are believed to inhibit hemozoin formation by binding to heme subunits, either by adsorbing to the fastest-growing face of the crystal or by forming a heme-drug complex [65,66]. This results in a build-up of free heme which is toxic and threatens parasite survival. In this study, β-hematin (synthetic hemozoin) formation was monitored using NP-40, which is a commercially available detergent used to create a neutral lipid environment, adept at promoting crystallisation under physiological conditions, similar to that of the malaria parasite's digestive vacuole [62,63]. β-Hematin inhibition was quantified by observing the formation of the heme-pyridine complex [67].

The results of the β-hematin inhibition assay for the above-mentioned compounds, amodiaquine (AQ) and chloroquine (CQDP) are shown in Table 3. Compounds **6a**, **6d**, **9a**, **9b**, and once again, **7a**, were found to be the most potent and were more active than the parent compound, AQ, exhibiting β-hematin inhibition activities of less than 4.02 μM. All of the screened compounds, except **7b** and **7c**, were found to be more active than the CQDP standard. Interestingly, **7b** and **7c** exhibited nanomolar asexual blood stage activity comparable to or greater than CQ, when tested against the chloroquine-sensitive NF54 strain of *P. falciparum* (Table 1). The relatively poorer β-hematin inhibitory activity of these two complexes, relative to CQ, suggests that these compounds are likely to have an alternative or additional mode of action, in addition to inhibiting hemozoin formation.

These results indicate that by incorporating the ferrocene moiety onto the amodiaquine scaffold enhances its ability to inhibit β-hematin formation under the conditions of this assay. The agreeable antiplasmodial and enhanced β-hematin inhibition activity are likely attributed to the hydrophobic nature of ferrocene, which equips it to readily interact with membranes and lipids. The amodiaquine scaffold

Table 2
Gametocytocidal activity of selected ferrodiaquines against immature and mature *P. falciparum* gametocytes.

Compound	[a]IC_{50} ± SD (μM)	
	Immature gametocytes (>90 % stage II/III)	Mature gametocytes (>95 % stage V)
6d	1.872 ± 0.549	>10
7a	1.272 ± 0.074	>10
7b	>20	>10

[a] IC_{50}, half-maximal inhibitory concentration determined in triplicate (n = 3).

Table 3
Experimental and *in silico* docking results of ferrodiaquines assessed for β-hematin inhibitory activity.

Compound	β-Hematin IC_{50} ± SD (μM)	Binding score (kcal/mol)
6a	3.17 ± 0.54	−13.91
6b	4.91 ± 1.01	−15.60
6c	n.d.	−14.66
6d	4.02 ± 0.20	−15.80
7a	3.92 ± 0.41	−14.06
7b	15.20 ± 1.82	−15.05
7c	14.97 ± 0.43	−13.84
7d	7.05 ± 0.54	−16.37
9a	3.37 ± 0.29	−13.09
9b	2.27 ± 0.41	−15.72
9c	5.43 ± 1.12	−16.79
AQ	4.48 ± 0.27	−13.98
CQDP	10.43 ± 0.30	n.d.

provides key structural characteristics which encourage strong heme binding which is optimal for β-hematin inhibition. Overall, the chlorinated amines (**9a** and **9b**) exhibited better inhibition activity when compared to the unchlorinated amines (**7a** and **7b**). This is likely owing to the presence of the 7-chloro group which is important for promoting β-hematin inhibition. This, in combination with the larger available planar surfaces, enhances β-hematin inhibition due to increased π-π interactions. Notably, compound **9b** was found to be the most active with an IC_{50} of 2.27 ± 0.41 μM; twice as active as the parent drug, AQ (Table 3). The activity of this compound is likely due to the presence of the 7-chloro group and the basic amino side chain, which increase the lipophilicity and thus promoting drug accumulation. Therefore, it can be proposed that the digestive vacuole is the likely site of localisation for this library of compounds, with hemozoin as the potential target.

2.4.2. Hemozoin molecular docking binding studies

Molecular docking simulations were performed to gain further insight into the possible mode of interaction and the binding affinity of the ferrodiaquines with hemozoin. This was realized *in silico* by constructing a 3 × 3 × 3 hemozoin unit cell from an experimentally resolved crystal structure of the macromolecule (CCDC code: XETXUP01) [68]. Docking simulations were conducted in AutoDock to study the interactions of the compounds with the fast-growing {001} face of the hemozoin crystal, purported as the preferred binding site for quinoline antiplasmodials to inhibit heme detoxification [69,70]. The results are reported in Table 3 as docking scores (in kcal/mol) of the minimum binding energy conformations of docked structural poses of the compounds on the crystal.

The docking scores suggest stable interactions between the hemozoin crystal and the compounds, with predicted minimum binding energies below −13 kcal/mol. Interestingly, a majority of the compounds had lower minimum binding energies than AQ, which is indicative of stronger interactions with hemozoin. With the exception of **9c**, all the analogues featuring the basic lateral dimethyl side chain, on the ferrocene unit, were consistently predicted to be more stable than their counterparts lacking this moiety (Table 3). This lends credence to the importance of this group in the activity of ferrodiaquines. Analysis of the intermolecular forces involved in hemozoin binding predicts π-π contacts as well as hydrophobic and electrostatic interactions as the primary modes of stabilization between the minimum energy conformation of the docked compound and the crystal in the bound complex (Fig. 2).

2.5. Aqueous and microsomal stability studies

The stability of bioactive compounds is a crucial parameter in their biological assessment. This is particularly so for organometallic complexes, as they may feature metallic centers that can coordinate water molecules, which can affect their activity (e.g. cisplatin) [71,72], and their distribution in the body, thus dictating their biological activity. Furthermore, biological systems consist of a complex matrix, rich not only in water but also in biological molecules which have the capacity to coordinate the metallic centers of organometallic complexes, giving similar biological consequences as water coordination. In the current study, it was important to ascertain the integrity and longevity of the investigated ferrodiaquines in an aqueous medium as well as biological models. Thus, the stability of the compounds was interrogated in PBS and mouse and microsomal models.

2.5.1. Aqueous stability in PBS

The aqueous stability of selected ferrodiaquines was spectrophotometrically assessed in an aqueous medium; PBS buffer at pH 7.4. A fixed concentration of the compound in DMSO was incubated in PBS and the UV–Vis spectrum was monitored over a period of 48 h. Changes in the spectrum by way of bathochromic or hypsochromic effects, post-incubation in the aqueous medium, implied modifications in the structural integrity of the compound, from which stability could be inferred. The results are illustrated in Fig. 3. The UV–Vis spectra of most of the compounds remained unaltered over 48 h, suggesting that they are relatively stable in aqueous media over this period.

2.5.2. Microsomal stability in mouse and human microsomes

The microsomal stability of selected ferrodiaquines was determined in mouse and human microsomes. Amides **9b** and **6d** showed higher stability in the human microsomes over mouse microsomes, while an opposite observation was made for **7d**, which lacks the amide functionality (Table 4). The reference drug **FQ** was generally longer lived compared to the ferrodiaquines in both microsome types, with superior half-lives and remaining at 27 and 45% levels after 30 min in human and mouse microsomes, respectively, post-incubation. Compound **6b** showed the lowest internal clearance (88.9 μL/min/mg) in the series, with human clearance lower than that of **FQ** (110 μL/min/mg). Likewise, the remaining levels of **6b** in human microsomes 30 min post incubation (35 %), as well as the half-life (20 min), are better than **FQ** (27 %, 16 min).

A quick interrogation of the structural effects on microsomal stability suggests that the amide bond slows down the metabolism of ferrodiaquines in human microsomes and is labile in mouse microsomes. The phenolic hydroxyl group appears to maintain a similar stability profile in both microsomes as observed in the comparable clearance values, half-lives, and remaining percentage levels of **6b** after 30 min. The

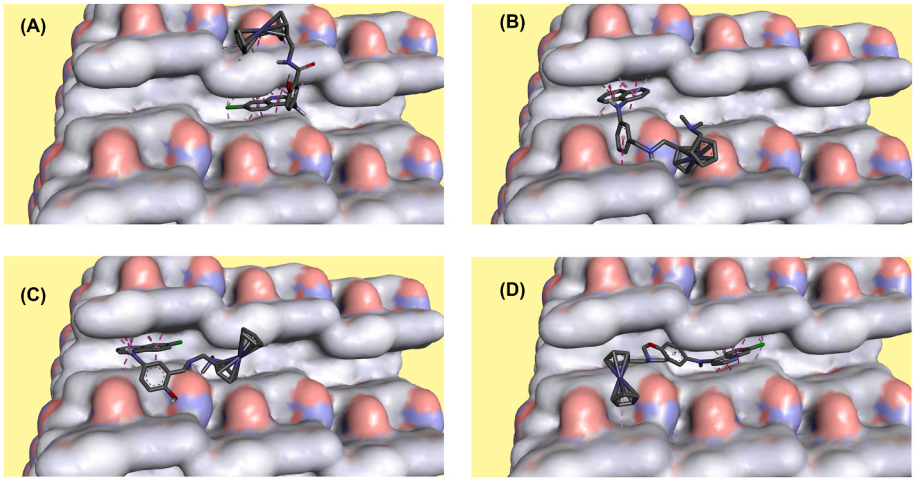

Fig. 2. Computational docking results showing minimum energy conformations of ferrodiaquines (**A**) *(S)*-**6b**, (**B**) *(S)*-**7d**, (**C**) *(S)*-**9b** and (**D**) **9c** interacting with the {001} fast-growing face of the hemozoin crystal.

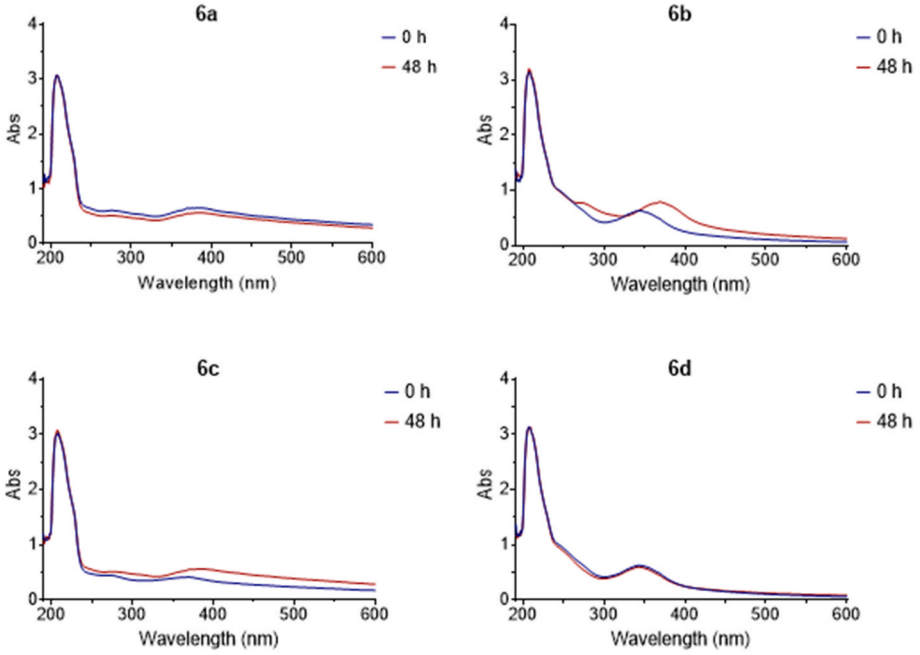

Fig. 3. Aqueous solubility of ferrodiaquines assessed by UV–Vis spectroscopy in PBS (pH 7.4) over 48 h.

Table 4
Stability of selected ferrodiaquines in human and mouse microsomes.

Compound	Species	Microsomal stability		
		% Remaining (30 min)	Half-life (min)	Cl_{int} (μL/min/mg)
6b	Mouse	32	18	94.4
	Human	35	20	88.9
6d	Mouse	8	8	213
	Human	20	13	135
7d	Mouse	37	21	83
	Human	6	8	230
FQ	Mouse	45	26	66
	Human	27	16	110

disconnect in stability of the compounds between the two microsomal types could be as a result of species-specific differences in CYP enzyme composition between humans and mice.

3. Conclusions

Using a bioorganometallic-drug hybridisation strategy, ferrocenylamodiaquine hybrid derivatives, i.e., ferrodiaquines, were synthesised. The antimalarial activity of the synthesized compounds was investigated using CQS NF54 and multidrug-resistant K1 *P. falciparum* strains. The compounds generally showed higher selectivity for the sensitive strain over the resistant strain, with most displaying activities higher than or comparable to the clinical antimalarial drug, CQ. Ferrodiaquine **7a** was the most potent compound among the tested compounds against both strains, displaying comparable activity in the two strains ($IC_{50} \approx 19$ nM), with an RI value < 1 and exceeding that of FQ. This suggests that the compound is able to retain its activity in the resistant strain and is thus not subject to the same resistance mechanism(s) developed in the multidrug-resistant strain. More notably, this compound was more potent than AQ in the resistant strain of the parasite. Ferrodiaquine **7a** also showed potential transmission-blocking properties by inhibiting the growth of stage II/III and stage V *P. falciparum* gametocytes. The multistage activity of this compound suggests that it can be used in not only the treatment of the disease but can play a role in preventing further transmission. Preliminary SAR analyses suggest that bioorganometallic drug hybridisation of AQ with the ferrocene unit enhances the biological performance of the resultant compounds. Preliminary investigations into plausible mechanisms of action confirmed the ability of the synthesized compounds to inhibit β-hematin formation, with complex **7a** displaying improved efficacy relative to AQ. This was further corroborated by *in silico* docking studies of the compounds with hemozoin. This study has also highlighted that the switch between the carbonyl and CH_2 group at the α-carbon of the lateral ring can play a crucial role in determining selectivity for the resistant strain.

4. Experimental

4.1. Instrumentation and general methods

All the reagents used in the study were purchased from Merck, Science World and KIMIX and were used as received without further purification. The benzoic acids (**1a**,**b**) and 4,7-dichloroquinoline (**3**) were purchased from Merk and ferrocenyl methylamines (**4a**,**b**) were synthesized from ferrocene carboxaldehyde and *N*,*N*-dimethylaminoferrocene according to reported literature methods [10]. Synthesis of aniline **2a** is described in the Supporting Information. All the solvents were used without further purification with the exception of anhydrous tetrahydrofuran which was purified by distillation over a sodium wire according to standard procedures [73]. The progress of the reactions was monitored by thin-layer chromatography (TLC) using aluminium plates coated with Merck silica-gel F_{254} and the spots were visualized under ultraviolet light (UV 254 and 366 nm). Crude samples of the compounds were purified by silica-gel column chromatography using Merck Kieselgel 60 Å: 70e230 (0.068–0.2 mm) silica gel mesh. Melting points were determined on a BÜCHI Melting Point B-540 apparatus and were reported uncorrected. Agilent HPLC 1260 equipped with an Agilent DAD 1260 UV/Vis detector and a X Bridge C18 column (2.5 μM, 50 mm × 3 mm) was used to determine the purity of the compounds. The compounds were eluted isocratically with 0.5 % Et_3N/MeOH in DCM. Nuclear magnetic resonance (NMR) spectra were acquired at 30 °C on Bruker Topspin GmbH 400 plus spectrometer (^1H at 400 MHz, $^{13}C\{^1H\}$ at 100 MHz) or Bruker 600 FT spectrometer (^1H at 600 MHz, $^{13}C\{^1H\}$ at 150 MHz). The infrared (IR) spectra were recorded on a PerkinElmer Spectrum 100 FT-IR spectrometer using Attenuated Total Reflectance

(ATR). High-resolution mass spectrometry (HRMS) data were recorded on Waters Synapt G2 Mass Spectrometer (Central Analytical Facility, Stellenbosch University) using the electrospray ionization (ESI) method set to positive ionization mode.

4.2. Chemistry

4.2.1. Synthesis of quinolinyl benzoic acids (5a,b) [44]

The known compounds **5a,b** were prepared following a modified literature method [42] and compare favourably with the reported data [74]. Aniline **1a** or **2a** (1.0 eq.) was dissolved in EtOH (15 mL) followed by the addition of 4,7-dichloroquinoline **3** (1.2 eq.). The resulting suspension was refluxed for 24 h. Disappearance of the aniline spot (TLC) indicated completion of the reaction. The formed light-yellow precipitate was cooled to room temperature and diluted with distilled water (25 mL) after which it was collected by suction filtration and successively washed with distilled water (25 mL), EtOH (25 mL), and air-dried to afford the desired compound. For compound **5b**, the carboxylic acid group was regenerated by refluxing the ester (**S5b**) from the previous step in 3:2:1 THF/MeOH/H_2O (10 mL) with NaOH (5.0 eq.) for a period of 6 h, after which the pH of the resulting mixture was adjusted to 2 using conc. aqueous HCl solution. The formed precipitate was isolated by filtration and air-dried to furnish compound **5b**.

5-((7-Chloroquinolin-4-yl)amino)-2-hydroxybenzoic acid (5a). Light-yellow solid: 6.00 g (97%). MP: 325.4–326.5 °C (Lit. > 250 °C). ^{1}H NMR (600 MHz, DMSO-d_6) δ 11.11 (s, 1H, NH), 8.83 (d, $^3J_{HH}$ = 9.2 Hz, 1H, H_5), 8.63 (d, $^3J_{HH}$ = 6.9 Hz, 1H, H_2), 8.17 (d, $^3J_{HH}$ = 2.2 Hz, 1H, H_8), 7.94 (d, $^3J_{HH}$ = 8.4 Hz, 1H, $H_{3'}$), 7.91 (dd, $^3J_{HH}$ = 9.1, $^4J_{HH}$ = 2.2 Hz, 1H, H_6), 7.14 (d, $^3J_{HH}$ = 7.0 Hz, 1H, H_3), 7.10 (d, $^3J_{HH}$ = 2.2 Hz, 1H, $H_{6'}$), 7.07 (dd, $^3J_{HH}$ = 8.4, $^4J_{HH}$ = 2.2 Hz, 1H, $H_{4'}$).

3-((7-Chloroquinolin-4-yl)amino)benzoic acid (5b). Light-yellow solid: 1.91 g (86%). MP: 369.4–369.8 °C (Lit. > 300 °C). ^{1}H NMR (400 MHz, DMSO-d_6) δ 11.32 (s, 1H, NH), 8.91 (d, $^3J_{HH}$ = 9.1 Hz, 1H, H_5), 8.55 (d, $^3J_{HH}$ = 7.0 Hz, 1H, H_2), 8.21 (d, $^3J_{HH}$ = 2.1 Hz, 1H, H_8), 8.01 (d, $^3J_{HH}$ = 2.3 Hz, 1H, $H_{2'}$), 7.97 (d, $^3J_{HH}$ = 7.6 Hz, 1H, $H_{6'}$), 7.88 (dd, $^3J_{HH}$ = 9.1, $^4J_{HH}$ = 2.1 Hz, 1H, H_6), 7.80–7.74 (m, 1H, $H_{4'}$), 7.70 (t, $^3J_{HH}$ = 7.8 Hz, 1H, $H_{5'}$), 6.86 (d, $^3J_{HH}$ = 7.0 Hz, 1H, H_3).

4.2.2. General procedure for synthesis of amides (6a,b) [46]

A mixture of quinolinyl benzoic acid **5a** (1.0 eq.), either ferrocenyl amine **4a** or **4b** (1.0 eq.) and DCC (1.2 eq.) in pyridine (2 mL) was irradiated at 80 °C under microwave conditions (200 W) in a sealed vial for 1 h after which it was cooled to room temperature. The reaction mixture was diluted with methanol (25 mL) and filtered through Celite to remove the insoluble urea side product of DCC. The filtrate was collected and dried *in vacuo* to furnish a crude product that was purified on silica gel column chromatography (5% MeOH/DCM (**6a**), 7:2:1:1 Hex/EtOAc/MeOH/Et_3N (**6b**)) to afford the title compound.

5-((7-Chloroquinolin-4-yl)amino)-N-ferrocenemethyl-2-hydroxybenzamide (6a). Yellow solid. 163.0 mg (40%). MP: 242.0–242.5 °C. ^{1}H NMR (600 MHz, DMSO-d_6) δ 12.74 (s, 1H, OH), 9.23 (s, 1H, NH), 8.89 (s, 1H, NH), 8.60 (d, $^3J_{HH}$ = 5.1 Hz, 1H, H_2), 8.37 (d, $^3J_{HH}$ = 9.0 Hz, 1H, H_5), 7.95 (d, $^4J_{HH}$ = 2.2 Hz, 1H, H_8), 7.87 (d, $^3J_{HH}$ = 8.6 Hz, 1H, H_6), 7.60 (dd, $^3J_{HH}$ = 8.9, $^4J_{HH}$ = 2.2 Hz, 1H, $H_{4'}$), 7.24 (d, $^3J_{HH}$ = 5.2 Hz, 1H, H_3), 6.88 (dd, $^3J_{HH}$ = 8.7, $^4J_{HH}$ = 2.1 Hz, 1H, $H_{3'}$), 6.85 (d, $^4J_{HH}$ = 2.2 Hz, 1H, $H_{6'}$), 4.26 (t, $^2J_{HH}$ = 1.8 Hz, 2H, FcH), 4.23 (d, $^3J_{HH}$ = 5.6 Hz, 2H, $H_{1''}$), 4.20 (s, 5H, FcH), 4.12 (t, $^3J_{HH}$ = 1.8 Hz, 2H, FcH); ^{13}C NMR (150 MHz, DMSO- d_6) δ 167.7, 161.0, 152.0, 149.6, 146.2, 145.7, 134.1, 129.3, 127.7, 125.4, 124.7, 119.2, 110.7, 110.2, 107.2, 105.0, 85.7, 68.3 (2C), 68.1 (5C), 67.4 (2C), 37.8. FT-IR (ATR, cm^{-1}): ν = 3251 (N–H, amide), 1624 (C=O, amide), 1189 (C–N, amide). HPLC purity >97 % (t_R = 1.748 min). HRMS (ESI$^+$) *m/z* calculated for $C_{27}H_{23}ClFeN_3O_2$: 512.0823, found 512.0826 [M+H]$^+$.

5-((7-Chloroquinolin-4-yl)amino)-N-(2-(N,N-dimethylamino)methyl) ferrocenemethyl-2-hydroxybenzamide (6b). Brown semi-solid. Yield: 256 mg (41%). ^{1}H NMR (400 MHz, DMSO-d_6) δ 9.21 (s, 1H, NH), 8.59 (d, $^3J_{HH}$ = 5.3 Hz, 1H, H_2), 8.36 (d, $^3J_{HH}$ = 9.0 Hz, 1H, H_5), 7.94 (d, $^4J_{HH}$ = 2.1 Hz, 1H, H_8), 7.66–7.53 (m, 2H, $H_{3'}$, H_6), 7.23 (d, $^3J_{HH}$ = 5.3 Hz, 1H, H_3), 6.90 (d, $^3J_{HH}$ = 8.4 Hz, 1H, $H_{4'}$), 6.84 (s, 1H, $H_{6'}$), 4.43 (d, $^2J_{HH}$ = 14.5 Hz, 1H, $H_{2''a}$), 4.26 (d, $^2J_{HH}$ = 14.5 Hz, 1H, $H_{2''b}$), 4.23 (br s, 1H, FcH), 4.18 (s, 1H, FcH), 4.14 (s, 5H, FcH), 4.06 (s, 1H, FcH), 3.76 (d, $^2J_{HH}$ = 12.7 Hz, 1H, $H_{1''a}$), 3.00 (d, $^2J_{HH}$ = 12.8 Hz, 1H, $H_{1''b}$), 2.15 (s, 6H, NMe_2); ^{13}C{^{1}H} NMR (100 MHz, DMSO) δ 167.1, 161.0, 152.0, 149.6, 146.2, 145.6, 134.1, 128.7, 127.7, 125.4, 124.6, 119.1, 110.7, 110.3, 107.3, 105.0, 84.8, 83.0, 70.4, 69.0 (5C), 68.8, 65.7, 56.9, 44.3, 36.8 (2C). FT-IR (ATR, cm^{-1}): ν = 3205 (N–H, amide), 1608 (C=O, amide), 1199 (C–N, amide). HPLC purity >99% (t_R = 1.839 min). HRMS (ESI$^+$) *m/z* calculated for $C_{30}H_{30}ClFeN_4O_2$: 569.1401, found 596.1404 [M+H]$^+$.

4.2.3. General procedure for synthesis of amides (6c,d)

Iodine (1.0 eq.), quinoline benzoic acid **5b** (1.0 eq.), and Et_3N (2.0 eq.) were successively added to a solution of $P(OEt)_3$ (1.0 eq.) in DCM (20 mL) on ice and the resulting mixture stirred at room temperature for 30 min under argon atmosphere. After 30 min, a solution of either ferrocenyl amine **4a** or **4b** (1.0 eq.) in DCM (5 mL) was added to the stirring reaction mixture and further stirred for 12–24 h. Following completion of the reaction (TLC), the resultant brown reaction mixture was diluted with DCM (25 mL) and successively washed with saturated NH_4Cl solution (25 mL), 5% NaOH solution (25 mL), and brine (25 mL). The organic layer was dried (Na_2SO_4) and the solvent removed under reduced pressure to afford a crude product that was purified on silica gel column chromatography (5% MeOH/DCM) to afford the title compound.

3-((7-Chloroquinolin-4-yl)amino)-N-ferrocenemethylbenzamide (6c). Light-yellow solid: 282 mg (41%). MP: 186.9–188.2 °C. ^{1}H NMR (600 MHz, $CDCl_3$/MeOD-d_4) δ 8.23 (m, 2H, H_5, H_2), 7.90 (d, $^3J_{HH}$ = 2.2 Hz, 1H, H_8), 7.68 (t, $^3J_{HH}$ = 2.0 Hz, 1H, $H_{2'}$), 7.50 (d, $^3J_{HH}$ = 7.6 Hz, 1H, H_6), 7.46–7.42 (m, 1H, $H_{6'}$), 7.42–7.36 (m, 2H, $H_{4'}$, $H_{5'}$), 6.80 (d, $^3J_{HH}$ = 5.9 Hz, 1H, H_3), 4.29 (s, 2H, FcH), 4.27 (s, 2H, FcH), 4.17 (s, 5H, FcH), 4.13 (s, 2H, $H_{1''}$); ^{13}C{^{1}H} NMR (150 MHz, $CDCl_3$/MeOD-d_4) δ 166.7, 150.6, 148.0, 145.5, 139.3, 137.5, 136.2, 129.9, 127.0, 126.0, 125.0, 123.6, 123.6, 122.4, 117.5, 101.6, 84.7, 68.8 (7C), 68.5 (2C), 39.5. FT-IR (ATR, cm^{-1}): ν = 3383 (N–H, amide), 1646 (C=O, amide), 1133 (C–N, amide). HPLC purity >99% (t_R = 3.681 min). HRMS (ESI$^+$) *m/z* calculated for $C_{27}H_{23}ClFeN_3O$: 496.0874, found 496.0873 [M+H]$^+$.

3-((7-Chloroquinolin-4-yl)amino)-N-(2-(N,N-dimethylamino)methyl) ferrocenemethyl-benzamide (6d). Brown semi-solid: 290 mg (97%). ^{1}H NMR (600 MHz, $CDCl_3$) δ 9.07 (d, $^3J_{HH}$ = 8.9 Hz, 1H, H_5), 8.54 (d, $^3J_{HH}$ = 5.2 Hz, 1H, H_2), 8.03 (d, $^4J_{HH}$ = 2.2 Hz, 1H, H_8), 7.93 (d, $^3J_{HH}$ = 8.9 Hz, 1H, H_6), 7.78 (s, 1H, NH), 7.48–7.43 (m, 2H, H, $H_{2'}$, $H_{6'}$), 7.38–7.37 (m, 2H, $H_{4'}$, $H_{5'}$), 6.96 (br s, 1H, OH), 6.92 (d, $^3J_{HH}$ = 5.3 Hz, 1H, H_3), 4.75–4.71 (m, 1H, $H_{2''a}$), 4.25 (s, 1H, FcH), 4.19 (d, $^2J_{HH}$ = 14.4 Hz, 1H, $H_{2''b}$), 4.09 (s, 6H, FcH), 4.03 (t, $^2J_{HH}$ = 2.5 Hz, 1H, FcH), 3.84 (d, $^2J_{HH}$ = 12.7 Hz, 1H, $H_{1''a}$), 2.86 (d, $^2J_{HH}$ = 12.7 Hz, 1H, $H_{1''b}$), 2.14 (s, 6H, NMe_2); ^{13}C{^{1}H} NMR (100 MHz, $CDCl_3$) δ 165.7, 152.1, 149.9, 147.6, 140.2, 136.8, 135.5, 129.6, 129.2, 126.4, 125.0, 122.7, 122.2, 121.6, 118.4, 103.0, 84.6 (2C), 71.3, 70.6, 69.4 (5C), 66.2, 58.2, 44.8, 38.9 (2C). FT-IR (ATR, cm^{-1}): ν = 3237 (N–H, amide), 1739 (C=O, amide), 1217 (C–N, amide). HPLC >99% (t_R = 3.683 min). HRMS (ESI$^+$) *m/z* calculated for $C_{30}H_{30}ClFeN_4O$: 553.1452, found 553.1457 [M+H]$^+$.

4.2.4. General procedure for synthesis of amines (7a-d)

$LiAlH_4$ (5.0 eq.) was cautiously added to a solution of a relevant amide **6a-d** (1.0 eq) in anhydrous THF (25 mL) on ice. The resulting mixture was removed from the ice and then refluxed for 24–48 h under argon atmosphere. After completion of the reaction (TLC), excess $LiAlH_4$ was quenched by dropwise addition of brine (*ca.* 2 mL) until no fuming occurred. The yellow precipitate was diluted with DCM (50 mL) and removed over a pad of Celite by filtration, washing with excess DCM (3 × 25 mL) to ensure complete recovery of the product. The collected filtrate was successively washed with 5 % NaOH solution (20 mL) and

brine (25 mL) after which it was dried (K_2CO_3) and the solvent removed *in vacuo* to afford the crude product. The pure compound was isolated by column chromatography using deactivated basic alumina as the stationary phase (5% MeOH/DCM).

*N-(3-((((Ferrocene)methyl)amino)methyl)-4-hydroxyphenyl)quinolin-4-amine (**7a**)*. Brown semi-solid: 52.4 mg (75%). ^{1}H NMR (600 MHz, $CDCl_3$/MeOD-d_4) δ 8.50 (d, $^3J_{HH}$ = 5.4 Hz, 1H, H_2), 8.03 (d, J = 8.5 Hz, 1H, H_8), 7.91 (d, $^3J_{HH}$ = 8.4 Hz, 1H, H_5), 7.67 (t, $^3J_{HH}$ = 7.7 Hz, 1H, H_7), 7.49 (t, $^3J_{HH}$ = 7.7 Hz, 1H, H_6), 7.12 (dd, $^3J_{HH}$ = 8.4, $^4J_{HH}$ = 2.5 Hz, 1H, $H_{4'}$), 6.95 (d, $^4J_{HH}$ = 2.5 Hz, 1H, $H_{6'}$), 6.91 (d, $^3J_{HH}$ = 8.4 Hz, 1H, $H_{3'}$), 6.69–6.56 (m, 2H, H_3, NH), 4.17–4.11 (m, 9H, FcH), 4.01 (s, 2H, $H_{3''}$), 3.60 (s, 2H, $H_{2''}$); ^{13}C{^{1}H} NMR (150 MHz, $CDCl_3$/MeOD-d_4) δ 155.7, 149.9, 148.4, 147.9, 129.6, 129.1, 128.5, 124.8, 124.4, 124.2, 122.5, 118.5, 118.1, 116.6, 100.2, 83.8, 67.7 (5C), 67.5 (2C), 67.4 (2C), 50.8, 46.7. FT-IR (ATR, cm^{-1}): ν = 3075 (N–H, amine), 1196 (C–N, amine). HPLC purity >94% (t_R = 3.683 min). HRMS (ESI$^+$) *m/z* calculated for $C_{27}H_{26}FeN_3O$: 464.1420, found 464.1422 [M+H]$^+$.

*N-(3-((((2-((N,N-Dimethylamino)methyl)ferrocene)methyl)amino) methyl)-4-hydroxy-phenyl)quinolin-4-amine (**7b**)*. Yellow semi-solid: 80.0 mg (74%). ^{1}H NMR (400 MHz, $CDCl_3$/MeOD-d_4) δ 8.41 (d, $^3J_{HH}$ = 5.2 Hz, 1H, H_2), 8.10 (d, $^3J_{HH}$ = 8.4 Hz, 1H, H_5), 7.96 (d, $^3J_{HH}$ = 8.4 Hz, 1H, H_6), 7.65 (br s, 1H, H_7), 7.48 (br s, 1H, $H_{6'}$), 7.04 (d, $^3J_{HH}$ = 5.1 Hz, 1H, H_3), 6.97 (d, $^3J_{HH}$ = 7.9 Hz, 1H, $H_{3'}$), 6.87 (br s, 1H, H_8), 6.77 (d, $^3J_{HH}$ = 7.8 Hz, 1H, $H_{4'}$), 4.25 (s, 1H, FcH), 4.19 (s, 1H, FcH), 4.14–4.12 (m, 1H, $H_{3''a}$, FcH), 4.08 (s, 5H, FcH), 3.87 (d, $^2J_{HH}$ = 12.5 Hz, 2H, $H_{2''}$), 3.78 (d, $^2J_{HH}$ = 13.1 Hz, 1H, $H_{3''a}$), 3.57 (d, $^2J_{HH}$ = 13.5 Hz, 1H, $H_{1'b}$), 2.92 (d, $^2J_{HH}$ = 13.3 Hz, 1H, $H_{1'b}$), 2.17 (s, 6H, NMe_2); ^{13}C{^{1}H} NMR (150 MHz, $CDCl_3$/MeOD-d_4) δ 158.1, 149.0, 148.0, 147.2, 141.0, 130.0, 129.6, 127.8, 125.1, 120.3, 119.4, 115.8, 112.0, 109.8, 102.0, 82.6, 80.2, 71.2, 70.8, 69.0 (5C), 66.5, 57.3, 47.3, 45.2, 43.6 (2C). FT-IR (ATR, cm^{-1}): ν = 2925 (N–H, amine), 1171 (C–N, amine). HPLC purity >92% (t_R = 3.686 min). HRMS (ESI$^+$) *m/z* calculated for $C_{30}H_{32}FeN_4ONa$: 542.1898, found 542.1361 [M+Na]$^+$.

*N-(3-((((Ferrocene)methyl)amino)methyl)phenyl)quinolin-4-amine (**7c**)*. Brown semi-solid: 74.0 mg (33%). ^{1}H NMR (400 MHz, $CDCl_3$) δ 8.55 (d, $^3J_{HH}$ = 5.1 Hz, 1H, H_2), 8.04 (d, $^3J_{HH}$ = 8.4 Hz, 1H, H_8), 7.95 (d, $^3J_{HH}$ = 8.3 Hz, 1H, H_5), 7.68 (t, $^3J_{HH}$ = 7.6 Hz, 1H, H_7), 7.50 (t, $^3J_{HH}$ = 7.6 Hz, 1H, H_6), 7.36 (t, $^3J_{HH}$ = 7.6 Hz, 1H, $H_{5'}$), 7.30 (s, 1H, $H_{2'}$), 7.21 (d, $^3J_{HH}$ = 8.0 Hz, 1H, $H_{4'}$), 7.14 (d, $^3J_{HH}$ = 7.6 Hz, 1H, $H_{6'}$), 6.99 (d, $^3J_{HH}$ = 5.2 Hz, 1H, H_3), 4.20 (s, 2H, FcH), 4.14–4.07 (m, 7H, FcH), 3.84 (s, 2H, $H_{3''}$), 3.57 (s, 2H, $H_{1''}$); ^{13}C{^{1}H} NMR (100 MHz, $CDCl_3$) δ 150.8 (2C), 149.0, 147.7, 142.2, 140.2, 130.0, 129.8, 129.6, 125.5, 124.5, 122.3, 121.2, 119.9, 102.4, 86.4, 68.6 (7C), 68.0 (2C), 53.0, 48.5. FT-IR (ATR, cm^{-1}): ν = 3195 (N–H, amine), 1104 (C–N, amine). HPLC purity >98% (t_R = 3.695 min). HRMS (ESI$^+$) *m/z* calculated for $C_{27}H_{26}FeN_3$: 448.1471, found 448.1472 [M+H]$^+$.

*N-(3-((((2-((N,N-Dimethylamino)methyl)ferrocene)methyl)amino) methyl)-phenyl) quinolin-4-amine (**7d**)*. Brown semi-solid: 60.5 mg (38%). ^{1}H NMR (400 MHz, $CDCl_3$) δ 8.56 (d, $^3J_{HH}$ = 5.3, 1H, H_2), 8.03 (d, $^3J_{HH}$ = 8.4 Hz, 1H, H_8), 8.00 (d, $^3J_{HH}$ = 8.3 Hz, 1H, H_5), 7.68 (t, $^3J_{HH}$ = 7.6 Hz, 1H, H_7), 7.50 (t, $^3J_{HH}$ = 7.6 Hz, 1H, H_6), 7.37–7.31 (m, 2H, $H_{2'}$, $H_{5'}$), 7.25 (d, $^3J_{HH}$ = 7.2 Hz, 1H, $H_{4'}$) 7.07 (d, $^3J_{HH}$ = 8.1 Hz, 1H, $H_{6'}$), 7.01 (d, $^3J_{HH}$ = 5.3 Hz, 1H, H_3), 4.20 (s, 1H, FcH), 4.13 (s, 1H, FcH), 4.09–4.03 (m, 6H, FcH, $H_{3''a}$), 3.94 (d, $^3J_{HH}$ = 13.2 Hz, 1H, $H_{3''b}$), 3.79 (d, $^2J_{HH}$ = 13.4 Hz, 1H, $H_{2''a}$), 3.70 (d, $^2J_{HH}$ = 13.4 Hz, 1H, $H_{2''b}$), 3.43 (d, $^2J_{HH}$ = 13.2 Hz, 1H, $H_{1''a}$), 2.83 (d, $^2J_{HH}$ = 13.2 Hz, 1H, $H_{1''b}$), 2.09 (s, 6H, NMe_2); ^{13}C{^{1}H} NMR (100 MHz, $CDCl_3$) δ 150.9, 149.2, 147.6, 140.6, 140.5, 130.2, 129.7, 129.5, 125.5, 124.4, 122.5, 121.1, 120.1, 120.0, 102.5, 84.4, 83.7, 71.3, 70.7, 69.2 (5C), 66.3, 58.1, 51.8, 47.1, 44.8 (2C). FT-IR (ATR, cm^{-1}): ν = 3197 (N–H, amine), 1171 (C–N, amine). HPLC purity >99% (t_R = 3.678 min). HRMS (ESI$^+$) *m/z* calculated for $C_{30}H_{33}FeN_4$: 505.2049, found 505.2057 [M+H]$^+$.

4.2.5. Synthesis of quinolinyl phenol 8

Compound **8** was prepared from 4-hydroxyaniline **2b** (1.0 eq.) and 4,7-dichlroroquinoline **3** (1.2 eq.) following the procedure described for the synthesis of quinolinyl benzoic acids **5a**,**b**.

*4-((7-Chloroquinolin-4-yl)amino)phenol (**8**)*. Yellow solid: 3.27 g (96%). MP: 349.5–350.2 °C. ^{1}H NMR (300 MHz, DMSO-d_6) δ 11.06 (s, 1H, NH), 9.98 (s, 1H, OH), 8.84 (d, $^3J_{HH}$ = 9.2 Hz, 1H, H_5), 8.45 (d, $^3J_{HH}$ = 7.1 Hz, 1H, H_2), 8.15 (d, $^3J_{HH}$ = 2.1 Hz, 1H, H_8), 7.81 (dd, $^3J_{HH}$ = 9.1, $^4J_{HH}$ = 2.1 Hz, 1H, H_6), 7.30–7.20 (m, 2H, $H_{1'}$), 7.03–6.89 (m, 2H, $H_{2'}$), 6.61 (d, J = 7.0 Hz, 1H, H_3).

4.2.6. Synthesis of 7-chlorinated ferrodiaquines (9a-c)

A suspension of ferrocenyl amine **4b** (1.0 eq.) and paraformaldehyde (10.0 eq.) in EtOH (15 mL) and 1 mL Et_3N was heated under reflux for 30 min. This was followed by addition of quinolinyl phenol **8** (1.0 eq.) to the clear light-brown reaction solution from above. The resulting reaction mixture was further heated for 12 h after which it was cooled to room temperature. The cooled reaction mixture was diluted with DCM (50 mL) and successively washed with 1 M aq. NaOH solution (2 × 25 mL) and brine (25 mL). The DCM layer was dried over K_2CO_3 and the solvent removed *in vacuo* to give a brown residue, which was subjected to column chromatography on deactivated basic alumina (7:2:1:1 Hex/EtOAc/Et_3N/MeOH) to furnish the desired compounds (**9a-c**). The hydrolysis of **9c** to **9a** was achieved by refluxing **9c** (1.0 eq.) with 10% aq. citric acid (2 mL) in EtOH (10 mL) for 2 h at 75 °C after which the resulting yellow solution was cooled to room temperature and diluted with distilled H_2O (25 mL). The above solution was then washed with DCM (2 × 25 mL) and the aqueous layer collected. A solution of 38% aq. ammonium hydroxide (25 mL) was added to the collected aqueous layer and the product extracted with DCM (3 × 25 mL), dried (Na_2SO_2) and the solvent removed under reduced pressure to afford the pure compound (**9a**) in a yield of 37.8 mg (85% w.r.t. **9c**).

*7-Chloro-N-(3-((((ferrocene)methyl)amino)methyl)-4-hydroxyphenyl) quinolin-4-amine (**9a**)*. Brown semi-solid: 50.6 mg (7%). ^{1}H NMR (600 MHz, $CDCl_3$) δ 8.48 (d, $^3J_{HH}$ = 5.2 Hz, 1H, H_2), 8.01 (s, 1H, H_8), 7.84 (d, $^3J_{HH}$ = 8.6 Hz, 1H, H_5), 7.43 (d, $^3J_{HH}$ = 8.2 Hz, 1H, H_6), 7.11 (d, $^3J_{HH}$ = 8.4 Hz, 1H, $H_{4'}$), 6.94 (s, 1H, $H_{6'}$), 6.90 (d, $^3J_{HH}$ = 7.9 Hz, 1H, $H_{3'}$), 6.63 (d, $^3J_{HH}$ = 5.1 Hz, 1H, H_3), 6.54 (s, 1H, NH), 4.17 (s, 2H, FcH), 4.15 (s, 2H, FcH), 4.14 (s, 5H, FcH), 4.01 (s, 2H, $H_{3''}$), 3.60 (s, 2H, $H_{1''}$); ^{13}C{^{1}H} NMR (150 MHz, $CDCl_3$) δ 156.1, 151.5, 149.8, 149.4, 134.6, 130.4, 128.1, 125.3, 125.3, 125.0, 123.3, 122.6, 117.6, 116.9, 100.8, 84.7, 68.3 (5C), 67.9 (2C), 61.8 (2C), 59.0, 47.3. FT-IR (ATR, cm^{-1}): ν = 3078 (N–H, amine), 1199 (C–N, amine). HPLC purity >95% (t_R = 3.687 min). HRMS (ESI$^+$) *m/z* calculated for $C_{27}H_{25}ClFeN_3O$: 498.1030, found 498.1109 [M+H]$^+$.

*7-Chloro-N-(3-((((2-((N,N-Dimethylamino)methyl)ferrocene)methyl) amino)methyl)-4-hydroxyphenyl)quinolin-4-amine (**9b**)*. Brown semi-solid: 279.0 mg (46%). ^{1}H NMR (400 MHz, $CDCl_3$) δ 8.46 (d, $^3J_{HH}$ = 5.4 Hz, 1H, H_2), 7.98 (d, $^4J_{HH}$ = 2.1 Hz, 1H, H_8), 7.85 (d, $^3J_{HH}$ = 8.9 Hz, 1H, H_5), 7.40 (dd, $^3J_{HH}$ = 8.9, $^4J_{HH}$ = 2.2 Hz, 1H, H_6), 7.08 (dd, $^3J_{HH}$ = 8.4, $^4J_{HH}$ = 2.6 Hz, 1H, $H_{4'}$), 6.89–6.86 (m, 2H, $H_{3'}$, $H_{6'}$), 6.74 (s, 1H, NH), 6.64 (d, $^3J_{HH}$ = 5.4 Hz, 1H, H_3), 4.11 (d, J = 2.1 Hz, 1H, FcH), 4.09 (d, J = 2.3 Hz, 1H, FcH), 4.03 (s, 6H, FcH), 3.89–3.77 (m, 3H, $H_{2''a}$, $H_{3''}$), 3.74 (d, $^2J_{HH}$ = 12.5 Hz, 1H, $H_{1''a}$), 3.34 (d, $^2J_{HH}$ = 13.5 Hz, 1H, $H_{2''b}$), 2.75 (d, $^2J_{HH}$ = 12.5 Hz, 1H, $H_{1''b}$), 2.12 (s, 6H, NMe_2); ^{13}C{^{1}H} NMR (100 MHz, $CDCl_3$) δ 157.4, 152.0, 149.6, 149.5, 135.2, 129.8, 128.9, 125.8, 125.5, 125.4, 123.7, 121.3, 117.5, 117.4, 101.4, 84.2, 84.1, 71.5, 70.7, 69.1 (5C), 66.0, 58.4, 50.5, 46.0, 45.0 (2C). FT-IR (ATR, cm^{-1}): ν = 3190 (N–H, amine), 1168 (C–N, amine). HPLC purity >97% (t_R = 3.690 min). HRMS (ESI$^+$) *m/z* calculated for $C_{30}H_{32}ClFeN_4O$: 555.1609, found 555.1617 [M+H]$^+$.

N-(7-Chloroquinolin-4-yl)-3-(ferrocenemethyl)-3,4-dihydro-2H-benzo [e] [1,3]*oxazin-6-amine (**9c**)*. Light-brown solid: 95.4 mg (13%). MP: 209.3–210.6 °C. ^{1}H NMR (400 MHz, $CDCl_3$) δ 8.47 (d, $^3J_{HH}$ = 5.4 Hz, 1H, H_2), 8.01 (d, $^4J_{HH}$ = 2.0 Hz, 1H, H_8), 7.88 (d, $^3J_{HH}$ = 9.0 Hz, 1H, H_5), 7.43 (dd, $^3J_{HH}$ = 8.9, $^4J_{HH}$ = 2.1 Hz, 1H, H_6), 7.09 (dd, $^3J_{HH}$ = 8.5, $^4J_{HH}$ = 2.5 Hz, 1H, $H_{7'}$), 6.93 (d, $^4J_{HH}$ = 2.5 Hz, 1H, $H_{5'}$), 6.88 (d, $^3J_{HH}$ = 8.6 Hz, 1H, $H_{8'}$), 6.71 (d, $^3J_{HH}$ = 5.4 Hz, 1H, H_3), 4.86 (s, 2H, $H_{2'}$), 4.22 (t, $^3J_{HH}$ = 1.8 Hz, 2H, FcH), 4.16 (t, $^3J_{HH}$ = 1.8 Hz, 2H, FcH), 4.12 (s, 5H,

FcH), 3.99 (s, 2H, $H_{4'}$), 3.75 (s, 2H, $H_{2''}$); $^{13}C\{^1H\}$ NMR (100 MHz, $CDCl_3$) δ 152.7, 151.8, 149.6, 149.4, 135.9, 135.7, 131.9, 128.9, 126.4, 124.8, 124.2, 121.7, 118.1, 117.8, 101.9, 83.7, 82.2, 70.3 (2C), 69.1 (5C), 68.9 (2C), 51.6, 49.9. FT-IR (ATR, cm^{-1}): $\nu = 3073$ (N–H, amine), 1225 (C–O, oxazine), 1205 (C–N, oxazine), 1143 (C–N, amine). HPLC purity >95% (t_R = 3.690 min). HRMS (ESI^+) *m/z* calculated for $C_{28}H_{25}ClFeN_3O$: 510.1030, found 510.1033 $[M+H]^+$.

4.3. Biological evaluation

4.3.1. pLDH assay for blood stage antiplasmodial activity

The test samples were evaluated in triplicate, on two or three separate occasions, against both the CQ-sensitive (NF54) and CQ-resistant (K1) strains of the malaria parasite *P. falciparum*. Continuous i*n vitro* cultures of asexual erythrocyte stages of the parasite were maintained using a modified literature method of Trager and Jensen [75]. Quantitative assessment of the *in vitro* antiplasmodial activity was determined using the parasitic lactate dehydrogenase (pLDH) assay [54]. The test samples were prepared to a 20 mg/mL stock solution in 100 % DMSO. Stock solutions were stored at −20 °C. Further dilutions were prepared in complete medium on the day of the experiment. Samples **5a**, **5b**, and **9a** were tested as a suspension, as they were poorly soluble at the prepared concentration (20 mg/mL, Table 1). Chloroquine diphosphate (CQDP) was used as the reference drug. Samples were screened for initial activity at a concentration of 100 μg/mL. A full dose-response was performed to determine the concentration inhibiting 50% of parasite growth (IC_{50} value). Based on the results of the initial screening, test samples were tested at a starting concentration of either 100 μg/mL, 10 μg/mL, 5 μg/mL, or 1 μg/mL, which was then serially diluted 2-fold in complete medium to give 10 concentrations. The same dilution technique was used for all samples. The 50 % inhibitory concentration (IC_{50}) values were obtained from full dose-response curves, using a non-linear dose-response curve fitting analysis *via* GraphPad Prism v.5 software.

4.3.2. Gametocyte assay

The luciferase reporter assay was established to enable quantifiable investigations of the stage-specific action of gametocytocidal compounds for both immature and mature gametocytes using the marker cell line; NF54-*Pfs*16-GFP-Luc [76,77]. Drug assays were set up on day 5 and 13 (representing >90% of either immature stage II/III or >95 % mature stage V gametocytes, respectively). In each instance, assays were set up using a 2–3 % gametocytaemia, 1.5 % haematocrit culture and 48 h drug pressure under hypoxic conditions (90% N_2, 5% O_2, and 5% CO_2) at 37 °C, without shaking. Compounds are diluted 3-fold in at least a 9-point serial dilution series starting at 20 μM, with a non-lethal DMSO concentration of <0.1% maintained. Luciferase activity was determined in 30 μL parasite lysates by adding 30 μL luciferin substrate (Promega Luciferase Assay System) at room temperature and detection of resultant bioluminescence at an integration constant of 10 s with the GloMax®-Multi + Detection System with Instinct® Software. Methylene blue (5 μM) and internal project specific controls (MMV390048, 5 μM) are routinely included as controls. IC_{50} (concentration of compound required to inhibit viability of half of the cell population) was determined in GraphPad Prism with a non-linear regression fit with variable slope (4-parameter) on the dose-response data. All IC_{50} values are reported after three independent biological repeats (n = 3), each performed in technical triplicates, with data reported as average ± S.E. Assay quality parameters are evaluated for each assay, including Z′-factors (data quality compared to reproducibility using signal, noise and background parameters; accepted metric >0.6), regression (accepted r2 > 0.9); >80% viable parasites (top plateau); <20% killed parasites (bottom plateau), Hill slope ~1. Internal controls should perform at >90% inhibition for methylene blue and >70% inhibition for MMV390048.

4.3.3. β-Hematin inhibition assay

A modified method of the detergent mediated β-hematin inhibition assay as described by Carter et al. [63] was used to screen compounds of interest for β-hematin inhibition activity. Stock solutions of the test compounds were dissolved in 100 % DMSO to provide 20 mM solutions whereas the control compound (chloroquine diphosphate salt) was dissolved in 100 % MilliQ water to afford the same initial concentration. Twenty microlitres of the drug stock solutions were dispensed into column 12 of a 96-well microtitre plate in addition to 140 μL MilliQ water and 40 μL of NP40 detergent (305.5 μM). A solution comprising water/NP40 (305.5 μM)/DMSO at a v/v ratio of 70 %/20 %/10 % respectively was prepared after which 100 μL was dispensed into all wells in columns 1–11. A serial dilution of the drug solutions was performed by extracting 100 μL from column 12 until column 2 thereby creating a concentration range. Column 1 contained 0 mM of compound and therefore served as a blank. Plates were pre-read at 405 nm using a MultiSkan GO plate reader to allow for absorbance correction in the case of coloured compounds. A stock solution of hematin was freshly prepared prior to use by sonicating haemin in DMSO for 2 min after which 178.8 μL was suspended in 1 M acetate buffer (pH 4.8, 20 mL). This suspension was then vortexed and 100 μL was added to each well across columns 1–12 of the microtitre plate affording a final concentration of hematin in all wells of 100 μM. The plates were then covered and incubated for ~5 h at 37 °C in a temperature-controlled incubator.

Post-incubation, the unreacted hematin was quantified following the pyridine-ferrichrome method developed by Ncokazi and Egan [67]. Thirty-two microlitres of a 50 % (v/v) pyridine solution (acetone/-water/2 M HEPES buffer (pH 7.4)/pyridine at a v/v ratio of 20 %/20 %/10 %/50 % respectively) was added to all wells followed by 60 μL of pure acetone which encouraged the dispersion of hematin. Plates were read at 405 nm using the MultiSkan GO plate reader. The 50 % inhibitory concentration (IC50) for each compound was determined from the absorbance corrected values at 405 nm and analysed using the sigmoidal dose-response curve fit in GraphPad Prism v 9.0.0.

4.4. Aqueous stability studies in PBS buffer

For each compound, a UV–Vis spectrum of a 50 μM solution prepared in PBS buffer at pH 7.4 (<0.005 % DMSO (v/v) in the final volume) was acquired between 200 and 600 nm immediately after preparation. The solution was kept at ambient temperature for 48 h and the spectrum recorded. Spectral shifts between the spectra acquired pre- and post-incubation were analysed and aqueous stabilities inferred from observed changes observed or lack of.

4.5. Microsomal stability studies

Solubility was measured at pH 7.4 using an adapted miniaturised shake-flask method, in 96-well plate format [78,79]. Briefly 4 μl of a 10 mM stock in DMSO was added to a 96-well plate and evaporated using a GeneVac system. Phosphate buffer at pH 7.4 was then added to the wells and the plate was incubated for 24 h at 25 °C with shaking. At the end of the incubation, the samples were centrifuged at 3500 g for 15 min then transferred to an analysis plate. A calibration curve in DMSO for each sample between 10–220 μM was prepared and included in the analysis plate. Analysis was then performed by HPLC-DAD and solubility of each sample determined from the corresponding calibration curve. The microsomal stability assay was performed using a single-point assay design [80]. Briefly, the compounds were incubated at 1 μM in human (mixed gender, Xenotech), Rat (male rat IGS, Xenotech) and mouse (male mouse CD1, Xenotech) liver microsomes (0.4 mg/ml) for 30 min at 37 °C. Reactions were quenched by adding ice-cold acetonitrile containing internal standard. The samples were then centrifuged. Afterwards the samples were analysed via LC-MS/MS for the disappearance of parent compound. Half-life and clearance were determined using standard equations [80,81].

4.6. Molecular docking studies against hemozoin crystal

The structures of the compounds were prepared using BIOVIA Discovery Studio Client 2016 (Dassault Systèmes BIOVIA Discovery Studio Client 2016 v16.1.0.15350, San Diego: Dassault Systèmes, 2016) and their energies minimized in Chem3D 18.2 (Chem3D v18.2.0.48, PerkinElmer, 2019) applying a RMS gradient of 0.100. BIOVIA Materials Studio 2017 software package (Dassault Systèmes BIOVIA Materials Studio 2017 v17.1.0.48, San Diego: Dassault Systèmes, 2017) was used to generate a 3 × 3 × 3 hemozoin crystal cell unit as previously described [82]. The docking simulations were carried out in the AutoDock Interface in Chem3D 18.2 (Chem3D v18.2.0.48, PerkinElmer, 2019). The docking volume was defined by choosing centroid coordinates of (x, y, z) = (18.00, 21.00, 2.00) with grid point numbers (x, y, z) = (100.00, 120.00, 85.00) and spacing of 0.375 Å, covering the fast-growing {001} face of the crystal. The simulations were performed with a population size of 50, 27 × 10^3 generations and 250 × 10^3 energy evaluations, giving an output of 4 docked conformations for each compound. The results were reported in kcal/mol as docking score and the graphics were processed in BIOVIA Discovery Studio Client 2016 (Dassault Systèmes BIOVIA Discovery Studio Client 2016 v16.1.0.15350, San Diego: Dassault Systèmes, 2016).

CRediT authorship contribution statement

Mziyanda Mbaba: Writing – original draft, Validation, Investigation, Formal analysis, Data curation. **Taryn M. Golding:** Writing – review & editing, Investigation. **Reinner O. Omondi:** Writing – review & editing, Software, Investigation. **Roxanne Mohunlal:** Writing – review & editing, Investigation. **Timothy J. Egan:** Supervision, Resources. **Janette Reader:** Investigation, Data curation. **Lyn-Marie Birkholtz:** Writing – review & editing, Resources, Investigation. **Gregory S. Smith:** Writing – review & editing, Supervision, Resources, Project administration, Investigation, Funding acquisition, Conceptualization.

Declaration of competing interest

The authors declare that they have no known competing financial interests or personal relationships that could have appeared to influence the work reported in this paper.

Data availability

Data will be made available on request.

Acknowledgments

We gratefully acknowledge and thank the University of Cape Town and the National Research Foundation of South Africa (UID:129288) for financial support. The University of Cape Town (UCT) Drug Discovery and Development Centre (H3D) is also thanked for their assistance with solubility and stability studies. LMB acknowledges the South African Medical Research Council, Medicines for Malaria Venture (LMB: RD-19-001), and the Department of Science and Innovation South African Research Chairs Initiative Grants managed by the National Research Foundation (LMB UID: 84627).

Appendix A. Supplementary data

Supplementary data to this article can be found online at https://doi.org/10.1016/j.ejmech.2024.116429.

References

[1] M.d. Oliveira Pedrosa, R.M. Duarte da Cruz, J.d. Oliveira Viana, R.O. de Moura, H. M. Ishiki, J.M. Barbosa Filho, M.F. Diniz, M.T. Scotti, L. Scotti, F.J. Bezerra Mendonca, Hybrid compounds as direct multitarget ligands: a review, Curr. Top. Med. Chem. 17 (2017) 1044–1079.
[2] E. Proschak, H. Stark, D. Merk, Polypharmacology by design: a medicinal chemist's perspective on multitargeting compounds, J. Med. Chem. 62 (2018) 420–444.
[3] C. Herrera Acevedo, L. Scotti, M.F. Alves, M. de Ffm Diniz, M. Tullius Scotti, Hybrid compounds in the search for alternative chemotherapeutic agents against neglected tropical diseases, Lett. Org. Chem. 16 (2019) 81–92.
[4] A. Kumari, M. Karnatak, D. Singh, R. Shankar, J.L. Jat, S. Sharma, D. Yadav, R. Shrivastava, V.P. Verma, Current scenario of artemisinin and its analogues for antimalarial activity, Eur. J. Med. Chem. 163 (2019) 804–829.
[5] M. Patra, G. Gasser, The medicinal chemistry of ferrocene and its derivatives, Nat. Rev. Chem 1 (2017) 1–12.
[6] A. Singh, I. Lumb, V. Mehra, V. Kumar, Ferrocene-appended pharmacophores: an exciting approach for modulating the biological potential of organic scaffolds, Dalton Trans. 48 (2019) 2840–2860.
[7] L.K. Batchelor, P.J. Dyson, Extrapolating the fragment-based approach to inorganic drug discovery, Trends in Chemistry 1 (2019) 644–655.
[8] C.N. Morrison, K.E. Prosser, R.W. Stokes, A. Cordes, N. Metzler-Nolte, S.M. Cohen, Expanding medicinal chemistry into 3D space: metallofragments as 3D scaffolds for fragment-based drug discovery, Chem. Sci. 11 (2020) 1216–1225.
[9] S. Top, J. Tang, A. Vessières, D. Carrez, C. Provot, G. Jaouen, Ferrocenyl hydroxytamoxifen: a prototype for a new range of oestradiol receptor site-directed cytotoxics, Chem. Commun. (1996) 955–956.
[10] C. Biot, G. Glorian, L.A. Maciejewski, J.S. Brocard, O. Domarle, G. Blampain, P. Millet, A.J. Georges, H. Abessolo, D. Dive, Synthesis and antimalarial activity in vitro and in vivo of a new ferrocene– chloroquine analogue, J. Med. Chem. 40 (1997) 3715–3718.
[11] G. Jaouen, A. Vessières, S. Top, Ferrocifen type anti cancer drugs, Chem. Soc. Rev. 44 (2015) 8802–8817.
[12] F. Dubar, J. Khalife, J. Brocard, D. Dive, C. Biot, Ferroquine, an ingenious antimalarial drug–thoughts on the mechanism of action, Molecules 13 (2008) 2900–2907.
[13] D. Dive, C. Biot, Ferroquine as an oxidative shock antimalarial, Curr. Top. Med. Chem. 14 (2014) 1684–1692.
[14] W.E. Butler, P.N. Kelly, A.G. Harry, R. Tiedt, B. White, R. Devery, P.T. Kenny, The synthesis, structural characterization and biological evaluation of N-(ferrocenylmethyl amino acid) fluorinated benzene-carboxamide derivatives as potential anticancer agents, Appl. Organomet. Chem. 27 (2013) 361–365.
[15] S.B. Deepthi, R. Trivedi, L. Giribabu, P. Sujitha, C.G. Kumar, Palladium (II) carbohydrate complexes of alkyl, aryl and ferrocenyl esters and their cytotoxic activities, Inorg. Chim. Acta. 416 (2014) 164–170.
[16] N. Baartzes, C. Szabo, M. Cenariu, F. Imre-Lucaci, S.A. Dorneanu, E. Fischer-Fodor, G.S. Smith, In vitro antitumour activity of two ferrocenyl metallodendrimers in a colon cancer cell line, Inorg. Chem. Commun. 98 (2018) 75–79.
[17] C. Biot, W. Daher, N. Chavain, T. Fandeur, J. Khalife, D. Dive, E. De Clercq, Design and synthesis of hydroxyferroquine derivatives with antimalarial and antiviral activities, J. Med. Chem. 49 (2006) 2845–2849.
[18] Y. Li, C. de Kock, P.J. Smith, K. Chibale, G.S. Smith, Synthesis and evaluation of a carbosilane congener of ferroquine and its corresponding half-sandwich ruthenium and rhodium complexes for antiplasmodial and β-hematin inhibition activity, Organometallics 33 (2014) 4345–4348.
[19] T. Stringer, L. Wiesner, G.S. Smith, Ferroquine-derived polyamines that target resistant Plasmodium falciparum, Eur. J. Med. Chem. 179 (2019) 78–83.
[20] J.-P. Monserrat, R.I. Al-Safi, K.N. Tiwari, L. Quentin, G.G. Chabot, A. Vessières, G. Jaouen, N. Neamati, E.A. Hillard, Ferrocenyl chalcone difluoridoborates inhibit HIV-1 integrase and display low activity towards cancer and endothelial cells, Bioorg. Med. Chem. Lett. 21 (2011) 6195–6197.
[21] H. Bjelosevic, I.A. Guzei, L.C. Spencer, T. Persson, F.H. Kriel, R. Hewer, M.J. Nell, J. Gut, C.E. van Rensburg, P.J. Rosenthal, Platinum (II) and gold (I) complexes based on 1, 1′-bis (diphenylphosphino) metallocene derivatives: synthesis, characterization and biological activity of the gold complexes, J. Organomet. Chem. 720 (2012) 52–59.
[22] R. Aneja, A.A. Rashad, H. Li, R.V. Kalyana Sundaram, C. Duffy, L.D. Bailey, I. Chaiken, Peptide triazole inactivators of HIV-1 utilize a conserved two-cavity binding site at the junction of the inner and outer domains of Env gp120, J. Med. Chem. 58 (2015) 3843–3858.
[23] K. Kumar, S. Carrere-Kremer, L. Kremer, Y. Guerardel, C. Biot, V. Kumar, 1 H-1, 2, 3-triazole-tethered isatin–ferrocene and isatin–ferrocenylchalcone conjugates: synthesis and in vitro antitubercular evaluation, Organometallics 32 (2013) 5713–5719.
[24] T. Stringer, R. Seldon, N. Liu, D.F. Warner, C. Tam, L.W. Cheng, K.M. Land, P. J. Smith, K. Chibale, G.S. Smith, Antimicrobial activity of organometallic isonicotinyl and pyrazinyl ferrocenyl-derived complexes, Dalton Trans. 46 (2017) 9875–9885.
[25] World Malaria Report, World Health Organization, 2023.
[26] M. Adjuik, P. Agnamey, A. Babiker, S. Borrmann, P. Brasseur, M. Cisse, F. Cobelens, S. Diallo, J. Faucher, P. Garner, Amodiaquine-artesunate versus amodiaquine for uncomplicated Plasmodium falciparum malaria in African children: a randomised, multicentre trial, Lancet 359 (2002) 1365–1372.
[27] F. Nosten, N.J. White, Artemisinin-based combination treatment of falciparum malaria, Am. J. Trop. Med. Hyg. 77 (2007) 181–192.
[28] L. Ndung'u, B. Langat, E. Magiri, Amodiaquine resistance in Plasmodium berghei is associated with PbCRT His95Pro mutation, loss of chloroquine, artemisinin and primaquine sensitivity, and high transcript levels of key transporters, Wellcome Open Res. 2 (2017) 44.

[29] W.H. Organization, WHO Status Reports on Artemisinin Resistance and ACT Efficacy, World Health Organization, Geneva, Switzerland, 2019.
[30] N. Wasi, H. Singh, A. Gajanana, A. Raichowdhary, Synthesis of metal complexes of antimalarial drugs and in vitro evaluation of their activity against plasmodium falciparum, Inorg. Chim. Acta. 135 (1987) 133–137.
[31] N. Wasi, H. Singh, Coordination complexes of drugs-preparation and characterisation of metal complexes of amodiaquine-an antimalarial drug, Synth. React. Inorg. Met. Org. Chem. 18 (1988) 473–485.
[32] E. Enemose, E. Akporhonor, B. Kpomah, Preparation and evaluation of mixed-ligand complexes of Cu (II) and Co (II) with amodiaquine hydrochloride and sulphamethazine, J. Appl. Sci. Environ. Manag. 22 (2018) 933–936.
[33] L. Colina-Vegas, M.d.C.B. Silva, C.d.S. Pereira, A.I. Barros, J.A. Nobrega, M. Navarro, M. Rottmann, S. D'Alessandro, N. Basilico, A.A. Batista, D.R. M. Moreira, Antimalarial agents derived from metal-amodiaquine complexes with activity in multiple stages of the plasmodium life cycle, Chem. Eur J. 29 (2023) e202301642.
[34] O.V. Miroshnikova, T.H. Hudson, L. Gerena, D.E. Kyle, A.J. Lin, Synthesis and antimalarial activity of new isotebuquine analogues, J. Med. Chem. 50 (2007) 889–896.
[35] D.S. Ongarora, J. Gut, P.J. Rosenthal, C.M. Masimirembwa, K. Chibale, Benzoheterocyclic amodiaquine analogues with potent antiplasmodial activity: synthesis and pharmacological evaluation, Bioorg. Med. Chem. Lett. 22 (2012) 5046–5050.
[36] A.R. Parhizgar, A. Tahghighi, Introducing new antimalarial analogues of chloroquine and amodiaquine: a narrative review, Iran. J. Med. Sci. 42 (2017) 115.
[37] J. Okombo, C. Brunschwig, K. Singh, G.A. Dziwornu, L. Barnard, M. Njoroge, S. Wittlin, K. Chibale, Antimalarial pyrido [1, 2-a] benzimidazole derivatives with Mannich base side chains: synthesis, pharmacological evaluation, and reactive metabolite trapping studies, ACS Infect. Dis. 5 (2019) 372–384.
[38] K.A. Neftel, W. Woodtly, M. Schmid, P.G. Frick, J. Fehr, Amodiaquine induced agranulocytosis and liver damage, Br. Med. J. 292 (1986) 721–723.
[39] S. Tafazoli, P.J. O'Brien, Amodiaquine-induced oxidative stress in a hepatocyte inflammation model, Toxicology 256 (2009) 101–109.
[40] D.J. Naisbitt, D.P. Williams, P.M. O'Neill, J.L. Maggs, D.J. Willock, M. Pirmohamed, B.K. Park, Metabolism-dependent neutrophil cytotoxicity of amodiaquine: a comparison with pyronaridine and related antimalarial drugs, Chem. Res. Toxicol. 11 (1998) 1586–1595.
[41] S. Shimizu, R. Atsumi, K. Itokawa, M. Iwasaki, T. Aoki, C. Ono, T. Izumi, K. Sudo, O. Okazaki, Metabolism-dependent hepatotoxicity of amodiaquine in glutathione-depleted mice, Arch. Toxicol. 83 (2009) 701.
[42] P.M. O'Neill, A. Mukhtar, P.A. Stocks, L.E. Randle, S. Hindley, S.A. Ward, R. C. Storr, J.F. Bickley, I.A. O'Neil, J.L. Maggs, Isoquine and related amodiaquine analogues: a new generation of improved 4-aminoquinoline antimalarials, J. Med. Chem. 46 (2003) 4933–4945.
[43] P.M. O'Neill, B.K. Park, A.E. Shone, J.L. Maggs, P. Roberts, P.A. Stocks, G. A. Biagini, P.G. Bray, P. Gibbons, N. Berry, Candidate selection and preclinical evaluation of N-tert-butyl isoquine (GSK369796), an affordable and effective 4-aminoquinoline antimalarial for the 21st century, J. Med. Chem. 52 (2009) 1408–1415.
[44] S. Gemma, C. Camodeca, M. Brindisi, S. Brogi, G. Kukreja, S. Kunjir, E. Gabellieri, L. Lucantoni, A. Habluetzel, D. Taramelli, Mimicking the intramolecular hydrogen bond: synthesis, biological evaluation, and molecular modeling of benzoxazines and quinazolines as potential antimalarial agents, J. Med. Chem. 55 (2012) 10387–10404.
[45] C.S. Keenan, S.S. Murphree, Rapid and convenient conversion of nitroarenes to anilines under microwave conditions using nonprecious metals in mildly acidic medium, Synth. Commun. 47 (2017) 1085–1089.
[46] M. Mbaba, L.M. Dingle, T. Swart, D. Cash, D. Laming, D. Taylor, H.C. Hoppe, C. Biot, A.L. Edkins, S.D. Khanye, The in vitro antiplasmodial and antiproliferative activity of new ferrocene-based α-aminocresols targeting hemozoin inhibition and DNA interaction, Chembiochem 21 (2020) 2643–2658.
[47] P.-J. Chen, H.-Y. Wang, A.-Y. Peng, A mild and efficient amide formation reaction mediated by P (OEt) 3 and iodine, RSC Adv. 5 (2015) 94328–94331.
[48] B. Thiedemann, C.M. Schmitz, A. Staubitz, Reduction of N-allylamides by LiAlH4: unexpected attack of the double bond with mechanistic studies of product and byproduct formation, J. Org. Chem. 79 (2014) 10284–10295.
[49] B. Ravinder, S.R. Reddy, A.P. Reddy, R. Bandichhor, Amide activation by TMSCl: reduction of amides to amines by LiAlH4 under mild conditions, Tetrahedron Lett. 54 (2013) 4908–4913.
[50] S.-H. Xiang, J. Xu, H.-Q. Yuan, P.-Q. Huang, Amide activation by Tf2O: reduction of amides to amines by NaBH4 under mild conditions, Synlett 2010 (2010) 1829–1832.
[51] W. Burke, C.W. Stephens, Monomeric products from the condensation of phenol with formaldehyde and primary amines, J. Am. Chem. Soc. 74 (1952) 1518–1520.
[52] D. Marquarding, H. Klusacek, G. Gokel, P. Hoffmann, I. Ugi, Stereoselective syntheses. VI. Correlation of central and planar chirality in ferrocene derivatives, J. Am. Chem. Soc. 92 (1970) 5389–5393.
[53] C. Pi, X. Cui, X. Liu, M. Guo, H. Zhang, Y. Wu, Synthesis of ferrocene derivatives with planar chirality via palladium-catalyzed enantioselective C–H bond activation, Org. Lett. 16 (2014) 5164–5167.
[54] M. Makler, J. Ries, J. Williams, J. Bancroft, R. Piper, B. Gibbins, D. Hinrichs, Parasite lactate dehydrogenase as an assay for Plasmodium falciparum drug sensitivity, Am. J. Trop. Med. Hyg. 48 (1993) 739–741.
[55] T. Stringer, D. Taylor, C. de Kock, H. Guzgay, A. Au, S.H. An, B. Sanchez, R. O'Connor, N. Patel, K.M. Land, Synthesis, characterization, antiparasitic and cytotoxic evaluation of thioureas conjugated to polyamine scaffolds, Eur. J. Med. Chem. 69 (2013) 90–98.
[56] T.J. Egan, Quinoline antimalarials, Opin. Ther. Pat. 11 (2001) 185–209.
[57] H.D. Attram, S. Wittlin, K. Chibale, Incorporation of an intramolecular hydrogen bonding motif in the side chain of antimalarial benzimidazoles, Med. Chem. Commun. 10 (2019) 450–455.
[58] F. Dubar, T.J. Egan, B. Pradines, D. Kuter, K.K. Ncokazi, D. Forge, J.-F. Paul, C. Pierrot, H. Kalamou, J. Khalife, The antimalarial ferroquine: role of the metal and intramolecular hydrogen bond in activity and resistance, ACS Chem. Biol. 6 (2011) 275–287.
[59] C. Le Manach, J. Dam, J.G. Woodland, G. Kaur, L.P. Khonde, C. Brunschwig, M. Njoroge, K.J. Wicht, A. Horatscheck, T. Paquet, Identification and profiling of a novel diazaspiro [3.4] octane chemical series active against multiple stages of the human malaria parasite plasmodium falciparum and optimization efforts, J. Med. Chem. 64 (2021) 2291–2309.
[60] A. Horatscheck, A. Andrijevic, A.T. Nchinda, C. Le Manach, T. Paquet, L.P. Khonde, J. Dam, K. Pawar, D. Taylor, N. Lawrence, Identification of 2, 4-disubstituted imidazopyridines as hemozoin formation inhibitors with fast-killing kinetics and in vivo efficacy in the Plasmodium falciparum NSG mouse model, J. Med. Chem. 63 (2020) 13013–13030.
[61] C.L. Peatey, T.S. Skinner-Adams, M.W. Dixon, J.S. McCarthy, D.L. Gardiner, K. R. Trenholme, Effect of antimalarial drugs on Plasmodium falciparum gametocytes, J. Infect. Dis. 200 (2009) 1518–1521.
[62] R.D. Sandlin, M.D. Carter, P.J. Lee, J.M. Auschwitz, S.E. Leed, J.D. Johnson, D. W. Wright, Antimicrob. Agents Chemother. 55 (2011) 3363–3369.
[63] M.D. Carter, V.V. Phelan, R.D. Sandlin, B.O. Bachmann, D.W. Wright, Comb. Chem. High Throughput Screen. 13 (2010) 285–292.
[64] J.M. Combrinck, T.E. Mabotha, K.K. Ncokazi, M.A. Ambele, D. Taylor, P.J. Smith, H.C. Hoppe, T.J. Egan, Insights into the role of heme in the mechanism of action of antimalarials, ACS Chem. Biol. 8 (2013) 133.
[65] K.N. Olafson, M.A. Ketchum, J.D. Rimer, P.G. Vekilov, Mechanisms of hematin crystallization and inhibition by the antimalarial drug chloroquine, Proc. Natl. Acad. Sci. 112 (2015) 4946.
[66] D. Kuter, V. Streltsov, N. Davydova, G.A. Venter, K.J. Naidoo, T.J. Egan, Solution structures of chloroquine–ferriheme complexes modeled using MD simulation and investigated by EXAFS spectroscopy, J. Inorg. Biochem. 154 (2016) 114.
[67] K.K. Ncokazi, T.J. Egan, Anal. Biochem. 338 (2005) 306–319.
[68] D.S. Bohle, E.L. Dodd, P.W. Stephens, Structure of malaria pigment and related propanoate-linked metalloporphyrin dimers, Chem. Biodivers. 9 (2012) 1891–1902.
[69] R. Buller, M.L. Peterson, O. Almarsson, L. Leiserowitz, Quinoline binding site on malaria pigment crystal: a rational pathway for antimalaria drug design, Cryst. Growth Des. 2 (2002) 553–562.
[70] I. Weissbuch, L. Leiserowitz, Interplay between malaria, crystalline hemozoin formation, and antimalarial drug action and design, Chem. Rev. 108 (2008) 4899–4914.
[71] S. Dasari, P.B. Tchounwou, Cisplatin in cancer therapy: molecular mechanisms of action, Eur. J. Pharmacol. 740 (2014) 364–378.
[72] J.V. Burda, M. Zeizinger, J. Leszczynski, Hydration process as an activation of trans-and cisplatin complexes in anticancer treatment. DFT and ab initio computational study of thermodynamic and kinetic parameters, J. Comput. Chem. 26 (2005) 907–914.
[73] A.I. Vogel, B.S. Furniss, A.J. Hannaford, A.R. Tatchell, P.W.G. Smith, Vogel's Textbook of Practical Organic Chemistry, Longman Scientific & Technical, New York, United States, 1989.
[74] V.K. Agrawal, S. Sharma, Antiparasitic agents. Part VI. Synthesis of 7-chloro-4-(4-substituted-phenylamino)- and 7-chloro-4-(4-substituted-piperazin-1-yl)quinolines as potential antiparasitic agents, Indian J. Chem. 26B (1987) 550–555.
[75] W. Trager, J.B. Jensen, Human malaria parasites in continuous culture, Science 193 (1976) 673–675.
[76] J. Reader, M.E. van der Watt, L.M. Birkholtz, Streamlined and robust stage-specific profiling of gametocytocidal compounds against *Plasmodium falciparum*, Front. Cell. Infect. Microbiol. 12 (2022) 926460.
[77] J. Reader, M. Botha, A. Theron, S.B. Lauterbach, C. Rossouw, D. Engelbrecht, M. Wepener, A. Smit, D. Leroy, D. Mancama, T.L. Coetzer, Nowhere to hide: interrogating different metabolic parameters of Plasmodium falciparum gametocytes in a transmission blocking drug discovery pipeline towards malaria elimination, Malar. J. 14 (2015) 213.
[78] L. Zhou, L. Yang, S. Tilton, J. Wang, Development of high throughput equilibrium solubility assay using miniaturized shake-flask method in early drug discovery, J. Pharm. Sci. 96 (2007) 3052–3071.
[79] E. Kerns, L. Di (Eds.), Drug-like properties: concepts, structure, design and methods: from ADME to toxicity optimization, Academic Press (Elsevier Inc), 2008. ISBN: 978-0-1236-9520-8.
[80] L. Di, E. Kerns, N. Gao, S. Li, Y. Huang, J. Bourassa, D. Huryn, Experimental design on single-time-point high-throughput microsomal stability assay, J. Pharm. Sci. 93 (2004) 1537–1544.
[81] R.S. Obach, Prediction of human clearance of twenty-nine drugs from hepatic microsomal intrinsic clearance data: An examination of in vitro half-life approach and nonspecific binding to microsomes, Drug Metab. Dispos. 27 (1999) 1350–1359.
[82] F.P. L'abbate, R. Müller, R. Openshaw, J.M. Combrinck, K.A. de Villiers, R. Hunter, T.J. Egan, Hemozoin inhibiting 2-phenylbenzimidazoles active against malaria parasites, Eur. J. Med. Chem. 159 (2018) 243–254.